Ligand Field Effects in the Hydrated Divalent and Trivalent Metal Ions of the First and Second Transition Periods

Ralf Åkesson,† Lars G. M. Pettersson,*,‡ Magnus Sandström,*,† and Ulf Wahlgren‡

Contribution from the Department of Chemistry, Royal Institute of Technology, S-100 44 Stockholm, Sweden, and Department of Physics, Stockholm University, P.O. Box 6730, S-113 85 Stockholm, Sweden

Received October 12, 1993. Revised Manuscript Received February 4, 1994®

Abstract: The influence of d-shell occupation on the structure of the first hydration sphere for a series of hydrated transition metal ions has been evaluated by using theoretical calculations to optimize the geometry and find the conformations with lowest energy. General trends in the properties reflecting the calculated metal–oxygen bond strength and energy are discussed and compared with experimental values. The metal–oxygen distances, calculated by ab initio SCF methods using large basis sets for high-spin hexaaqua complexes in the T_h symmetry of the di- and trivalent 3d metal ions, follow closely the trends found in crystal structure determinations of the isomorphous series of the 3d hexaaqua metal ions in Tutton and alum salts. The variation of the binding energies in a hexaaqua complex shows the double-humped features expected for a splitting of the d orbitals in an octahedral ligand field with the largest stabilization at formal d^3 and d^8 electron configurations of the metal ions. In cases with degenerate d-orbitals, an additional splitting of the energy levels by a lowering of the symmetry of the hexahydrated ion will in some cases significantly increase the binding energy. For the largest d^1 and d^6 metal ions an "all-vertical", and for some large d^2 ions an "all-horizontal", conformation of the hydrogen atoms of the planarly coordinated water ligands around the trifold axis in the D_{3d} symmetry is favored. For the hexahydrated d^9 ion Ag^{2+}, the first-order Jahn–Teller effect leading to a tetragonal elongation of the octahedral coordination has been studied. The possibility that the nondistorted d^4 $[Cr(H_2O)_6]^{2+}$ complex is forced into a low-spin state in its hexafluorosilicate salt due to compression in the lattice has been considered. The electrostatically dominated binding in the hexaaqua complexes shows an increasing covalent contribution to the right in the transition rows, especially for the trivalent ions. The ligand field effects are generally larger for the trivalent than for the divalent ions and also larger for the $4d^n$ than for the $3d^n$ elements, although the overall bond strength is lower due to the larger size of the $4d^n$ ions. The high ligand field strength results in low-spin ground states for the hexahydrated Co^{3+}, Ru^{2+}, Rh^{3+} (d^6), and Ru^{3+} (d^5) ions in solution but, except for Rh^{3+}, these high- to low-spin transitions proved to be difficult to reproduce by computations for the isolated hexaaqua clusters. Electron correlation was introduced, but the effect of the surroundings, which also may provide an additional important contribution to the stabilization of the low-spin state, was not accounted for. The low-spin square-planar configurations of the d^8 complexes $[Pd(H_2O)_4]^{2+}$ and $[Ag(H_2O)_4]^{3+}$ are discussed in terms of ligand field effects.

Introduction

Hydrated Ions. This article continues our theoretical studies of hydrated transition metal ions, which previously have encompassed the binding energies and the dissociative water-exchange reactions of the hexahydrated divalent ions of the first transition period,[1] including the influence of Jahn–Teller effects in hexahydrated Cr^{2+}, Cu^{2+}, and Mn^{3+} ions.[2,3]

All the divalent ions, except Sc^{2+} and Ti^{2+}, and most of the trivalent ions of the first transition period exist as well-established high-spin hexahydrates in the solid state, although in aqueous solution hexaaqua complexes of the trivalent ions dominate only at low pH values due to their hydrolysis reactions.[4a] The Sc^{3+}, Cr^{3+}, Fe^{3+}, and Ga^{3+} ions are stable in the trivalent state, while Ti^{3+} and V^{3+} are easily oxidized.[4b,c] In solution the hexahydrated Co^{3+} ion oxidizes water and Mn^{3+} disproportionates, and their structures have thus only been studied in the solid state.[5]

In an octahedral ligand field, the five d orbitals of the metal ion are splitted into a triply degenerate $t_{2g}(O_h)$ and a doubly degenerate $e_g(O_h)$ set.[6] Almost regular octahedral coordination in hexaaqua complexes is found for all the above-mentioned trivalent 3d ions in cesium alum salts, $CsM(SO_4)_2 \cdot 12H_2O$,[5] even for the d^4 ion $[Mn(H_2O)_6]^{3+}$, where the expected Jahn–Teller distortion seemingly is suppressed in the high site-symmetry of the ion in the crystal structure in a way similar to that recently found also for the $[Cr(H_2O)_6]^{2+}$ (d^4) and $[Cu(H_2O)_6]^{2+}$ (d^9) ions in hexafluorosilicate structures.[7a,b] UV–vis spectra show that only for the d^6 Co^{3+} ion the ligand field is sufficiently strong in the hexaaqua complexes of the 3d ions to give a low-spin ground state (t_{2g}^6).[8]

When proceeding from the first to the second row of the d-block elements, several important changes of the electronic structure take place. In the present context, when di- and tripositive ions are treated, the dominating effect is the transition from a relatively

† Royal Institute of Technology.
‡ Stockholm University.
* Abstract published in *Advance ACS Abstracts,* June 15, 1994.

(1) (a) Åkesson, R.; Pettersson, L. G. M.; Siegbahn, P. E. M.; Sandström, M.; Wahlgren, U. *J. Phys. Chem.* **1992**, *96*, 10773. (b) *Ibid.* **1993**, *97*, 3765.
(2) Beagley, B.; Eriksson, A.; Lindgren, J.; Persson, I.; Pettersson, L. G. M.; Sandström, M.; Wahlgren, U.; White, E. W. *J. Phys.: Condens. Matter* **1989**, *1*, 2395.
(3) Åkesson, R.; Pettersson, L. G. M.; Sandström, M.; Wahlgren, U. *J. Phys. Chem.* **1992**, *96*, 150.
(4) (a) Burgess, J. In *Comprehensive Coordination Chemistry*; Wilkinson, G., Gillard, R. D., McCleverty, J. A., Eds.; Pergamon: Oxford, 1987; Vol. 2, Chapter 15.1. (b) McAuliffe, C. A.; Barratt, D. S. *Ibid. Vol.* 3, Chapter 31. (c) Vilas Boas, L. F.; Costa Pessoa, J. *Ibid. Vol.* 3, Chapter 33.
(5) (a) Beattie, J. K.; Best, S. P.; Skelton, B. W.; White, A. H. *J. Chem. Soc., Dalton Trans.* **1981**, 2105. (b) Best, S. P.; Forsyth, J. B.; Tregenna-Piggott, P. L. *Ibid.* **1993**, 2711.
(6) (a) Griffith, J. S. *The Theory of Transition-Metal Ions*; Cambridge University Press: Cambridge, England, 1971. (b) Douglas, B. E.; Hollingsworth, C. A. *Symmetry in Bonding and Spectra*; Academic Press: Orlando, FL, 1985; Chapter 8.
(7) (a) Cotton, F. A.; Falvello, L. R.; Murillo, C. A.; Quesada, J. F. *J. Solid State Chem.* **1992**, *96*, 192 and references therein. (b) Cotton, F. A.; Daniels, L. M.; Murillo, C. A.; Quesada, J. F. *Inorg. Chem.* **1993**, *32*, 4861. (c) Araya, M. A.; Cotton, F. A.; Daniels, L. M.; Falvello, L. R.; Murillo, C. A. *Ibid.* 4853. (d) Cotton, F. A.; Daniels, L. M.; Murillo, C. A. *Ibid*, 4868.
(8) Lever, A. B. P. *Inorganic Electronic Spectroscopy*, 2nd ed.; Elsevier: Amsterdam, 1984; Chapter 6.

0002-7863/94/1516-8691$04.50/0

compact 3d valence shell to the more spatially extended 4d shell. The interactions between the ligands and the more accessible 4d orbitals thus give increased ligand field splittings and a higher tendency toward low-spin complexes in the second transition row.[6] For the hydrated metal ions this is illustrated by the divalent low-spin (d^6) octahedral $[Ru(H_2O)_6]^{2+}$ [8-10] and the square-planar (d^8) $[Pd(H_2O)_4]^{2+}$ species,[11] which have no counterparts in the first transition period, and by the trivalent low-spin (d^5) $[Ru(H_2O)_6]^{3+}$ [5b,9,10,12a] and (d^6) $[Rh(H_2O)_6]^{3+}$ complexes.[13a,b] Another difference concerns the stability of the oxidation states and the formation of metal–metal bonds for the hydrated ions. In the first transition period monomeric divalent ions are common except for Sc and Ti, and apart from Ni, Cu, and Zn, also the +III state is known. In aqueous solution almost all of these ions are hexahydrated, except the d^0 ions Ca^{2+} and Sc^{3+}, which have higher hydration numbers because of their larger size.[1,14] For a tetrahedral ligand field the stabilization is highest for d^7 ions,[6] and in aqueous solution, a small amount of the tetrahydrate $[Co(H_2O)_4]^{2+}$ has been proposed to exist in equilibrium with the hexahydrate.[15] With the exception of the low-spin d^6 ion Co^{3+}, all the hydrated 3d ions have high-spin ground states,[8] which makes it easy to relate the calculated values to experimental results in discussions of periodic trends.

For the second transition series such comparisons are not equally straightforward because of the less uniform appearance of the hydrated di- and trivalent metal ions. At the start of the series the strontium(II) and yttrium(III) ions have a closed-shell (d^0) electron configuration but, due to their sizes, a larger hydration number in solution, probably 8.[16,17] Zirconium does not form any di- or trivalent aquo ions, and niobium(III) solutions in H_2SO_4 are strongly reducing.[18a,b] Hexaaquamolybdenum(III) ions crystallize in alum salts[18c,19] and can be obtained in fairly concentrated solutions, but in the divalent state, $[Mo_2(H_2O)_8]^{4+}$ species with a metal–metal bond are formed.[18d] Little is known of the uncommon technetium ions, although for the Tc^{2+} ion the single ion hydration enthalpy has been reported,[20] while the ruthenium(III) and rhodium(III) ions both form low-spin hexahydrated complexes with very slow water exchange in solution.[10,12a,21,22] Divalent $[Ru(H_2O)_6]^{2+}$ ions exist in aqueous solution,[10] while rhodium(II) is present as the dimeric complex $[Rh_2(H_2O)_{10}]^{4+}$ with a metal–metal bond.[23] Palladium(II) forms a square-planar low-spin $[Pd(H_2O)_4]^{2+}$ complex as shown by its electronic spectrum and substitution reactions,[11] but no trivalent ions are known. At the end of the second transition series, the d^{10} ions silver(I), cadmium(II), and indium(III) have stable oxidation states with well-defined $[Cd(H_2O)_6]^{2+}$ and $[In(H_2O)_6]^{3+}$ complexes.[16,17] The hydrated silver(I) ion probably forms a tetrahedral $[Ag(H_2O)_4]^{+}$ complex in solution.[17,24] The Jahn–Teller active (d^9) hydrated Ag^{2+} ion oxidizes water but has a transient existence at low pH.[25] No hydrated Ag(III) ions are known, although the $Ag(OH)_4^-$ complex exists in alkaline solution.[25]

Effects of Degeneracy. Distortions induced by first-order Jahn–Teller effects are strongest for high-spin d^4 and d^9 hexahydrated ions with an odd number of electrons in the two metal d orbitals directed toward the ligands, d_{z^2} and $d_{x^2-y^2}$. The vibronic coupling of $E\otimes e$ type,[26] which splits the two degenerate e_g orbitals in T_h symmetry (Figure 1a), has previously been investigated for Cu^{2+}, Cr^{2+}, and Mn^{3+}.[2,3] In the present work, the hexaaqua complex of the Ag^{2+} ion was studied in the same way by optimizing an axial (R_{ax}) and an equatorial (R_{eq}) metal–oxygen distance in D_{2h} symmetry in order to obtain the energy minima corresponding to the tetragonally elongated and compressed octahedral configurations. For several other of the presently investigated hexaaqua ions (e.g. Mo^{2+}, Tc^{3+}, Zn^{3+}, and Cd^{3+}), similar Jahn–Teller effects would also be expected. However, even if the Jahn–Teller effect can cause a large structural distortion of a hydrated cluster, our previous studies have shown that the energy gain and the change in the mean M–O distance are small,[1-3] and we have therefore not investigated its influence on the ions without known hexahydrates.

From structural studies on condensed phases it is also evident that the surroundings can have a large influence. In solution, hydrogen bonding of different strengths to the axial and equatorial water molecules is expected to increase the splitting,[2,3] while in the solid-state, crystallographic studies show varying degrees of distortion to the extreme of complete suppression of the Jahn–Teller effect for some Cr^{2+}, Cu^{2+}, and Mn^{3+} hexaaqua complexes in high-symmetry sites.[5,7] X-ray absorption studies also reveal significant differences in the distortion of hydrated Cu^{2+} ions in solution and in solid phases.[27] Even ligand field induced variations in the bond lengths can to some extent be influenced by the lattice, as shown by a recent comparison of precisely determined M–O distances from V^{2+} to Zn^{2+} in two isomorphous series of ammonium Tutton, $(NH_4)_2[M(H_2O)_6](SO_4)_2$, and hexafluorosilicate, $[M(H_2O)_6]SiF_6$, salts.[7b] In the latter series, with a more rigid high-symmetry lattice, the variation in the M–O distances is somewhat suppressed.

In a computational study using density functional theory on the hexaaqua clusters of the Cr^{2+}, Mn^{2+}, Fe^{2+}, Co^{2+}, Ni^{2+}, Cu^{2+}, and Zn^{2+} ions,[28a] small differences in M–O bond lengths were reported for the two differently oriented pairs of the equatorial water molecules for Cu^{2+} and Cr^{2+}, and also for the high-spin Fe^{2+} (d^6) and Co^{2+} (d^7) ions, which in principle also are Jahn–Teller unstable due to the uneven occupation of the degenerate $t_g(T_h)$ orbitals. No account of the energy gain relative to a regular conformation was given. The calculated bond lengths were in all cases much shorter (~0.1 Å) than our previous SCF results, and even shorter than the experimental mean distances. The basis set used for the water molecules was comparable to the

(9) Bernhard, P.; Bürgi, H.-B.; Hauser, J.; Lehmann, H.; Ludi, A. *Inorg. Chem.* **1982**, *21*, 3936. (b) Bernhard, P.; Ludi, A. *Inorg. Chem.* **1984**, *23*, 870.
(10) Brunschwig, B. S.; Creutz, C.; Macartney, D. H.; Sham, T.-K.; Sutin, N. *Faraday Discuss. Chem. Soc.* **1982**, *74*, 113.
(11) Hellquist, B.; Bengtsson, L. A.; Holmberg, B.; Hedman, B.; Persson, I.; Elding, L. I. *Acta Chem. Scand.* **1991**, *45*, 449.
(12) (a) Best, S. P.; Forsyth, J. B. *J. Chem. Soc., Dalton Trans.* **1990**, 395. (b) *Ibid.* **1990**, 3507. (c) *Ibid.* **1991**, 1721.
(13) (a) Armstrong, R. S.; Beattie, J. K.; Best, S. P.; Skelton, B. W.; White, A. H. *J. Chem. Soc., Dalton Trans* **1983**, 1973. (b) Best, S. P.; Beattie, J. K.; Armstrong, R. S. *Ibid.* **1984**, 2611. (c) Best, S. P.; Beattie, J. K.; Armstrong, R. S.; Braitwaite, G. P. *Ibid.* **1989**, 1771.
(14) (a) Kanno, H.; Yamaguchi, T.; Ohtaki, H. *J. Phys. Chem.* **1989**, *93*, 1695. (b) Kanno, H. *J. Phys. Chem.* **1988**, *92*, 4232.
(15) (a) Swift, T. J.; Connick, R. E. *J. Chem. Phys.* **1962**, *37*, 307. (b) Swift, T. J. *Inorg. Chem.* **1964**, *3*, 526. (c) Swaddle, T. W.; Fabes, L. *Can. J. Chem.* **1980**, *58*, 1418.
(16) Marcus, Y. *Chem. Rev.* **1988**, *88*, 1475.
(17) Johansson, G. *Adv. Inorg. Chem.* **1992**, *39*, 159.
(18) (a) Fay, R. C. In *Comprehensive Coordination Chemistry*; Wilkinson, G., Gillard, R. D., McCleverty, J. A., Eds.; Pergamon: Oxford, U.K., 1987; Vol. 3, Chapter 32. (b) Hubert-Pfalzgraf, L. G.; Postel, M.; Riess, J. G. *Ibid.* Chapter 34. (c) Sykes, A. G. *Ibid. Vol.* 3, Chapter 36.1. (d) Garner, C. D. *Ibid.* Vol. 3, Chapter 36.3.
(19) Brorson, M.; Gajhede, M. *Inorg. Chem.* **1987**, *26*, 2109.
(20) Smith, D. W. *J. Chem. Educ.* **1977**, *54*, 540.
(21) Read, M. C.; Sandström, M. *Acta Chem. Scand.* **1992**, *46*, 1177.
(22) Ducommun, Y.; Merbach, A. E. In *Inorganic High Pressure Chemistry, Kinetics and Mechanisms*; van Eldik, R., Ed.; Elsevier: Amsterdam, 1986; Chapter 2.1.
(23) Jardine, F. H. In *Comprehensive Coordination Chemistry*; Wilkinson, G., Gillard, R. D., McCleverty, J. A., Eds.; Pergamon: Oxford, U.K., 1987; Vol. 4, Chapter 48.5.
(24) Sandström, M.; Neilson, G. W.; Johansson, G.; Yamaguchi, T. *J. Phys. C* **1985**, *18*, L1115.
(25) Lancashire, R. J. In *Comprehensive Coordination Chemistry*; Wilkinson, G., Gillard, R. D., McCleverty, J. A., Eds.; Pergamon: Oxford, U.K., 1987; Vol. 5, Chapter 54.
(26) Bersuker, I. B.; Polinger, V. Z. *Vibronic Interactions in Molecules and Crystals*; Springer-Verlag: Berlin, 1989; Chapter 3.1.
(27) Carrado, K. A.; Wasserman, S. R. *J. Am. Chem. Soc.* **1993**, *115*, 3394.
(28) (a) Waizumi, K.; Ohtaki, H.; Masuda, H.; Fukushima, N.; Watanabe, Y. *Chem. Lett.* **1992**, 1489. (b) Fukushima, N.; Waizumi, K. *Chem. Express* **1993**, *8*, 265.

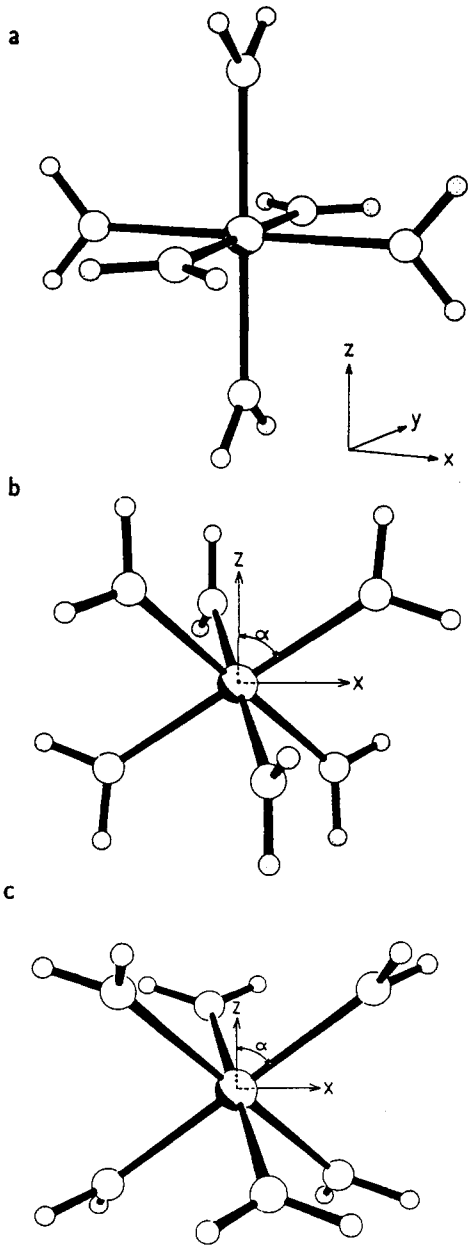

Figure 1. Hexahydrated metal ions with planarly coordinated water ligands in (a) T_h symmetry, (b) "all-vertical" D_{3d} symmetry, and (c) "all-horizontal" D_{3d} symmetry.

"medium-sized" basis set in our calculations, which gives an exaggerated dipole moment of the water molecules (see Table VI in ref 3). However, although we found a significant change in binding energy when optimizing the M–O distances with a large basis set on the SCF level (see Methods, below), only small increases (<0.02 Å) occurred in the bond length.[1] We made attempts in the present work to refine three different orthogonal pairs of M–O distances for Cu^{2+} and Fe^{2+} by SCF methods, but this resulted in insignificant lowering (<1 kJ mol^{-1}) of the previous binding energies. Recently, another similar unrestricted Hartree–Fock SCF study of a d^7 $[Co(H_2O)_6]^{2+}$ cluster gave consistent results with small changes in the Co–O distances (<0.005 Å) and the energy 1.3 kJ mol^{-1} lower than in the T_h symmetry.[29] Thus, the deviations in this density functional study[28a] are surprisingly large considering that nonlocal corrections were introduced, albeit only through perturbation theory. Recently, however, self-consistent determinations of the nonlocal correction terms were found to be important and led to an increase in the mean bond lengths by about 0.07 Å, and also changed the previously reported spurious Jahn–Teller distortions.[28b]

A more efficient mechanism for removing the degeneracy of the $t_g(T_h)$ d-orbitals can be provided by changing the orientation of the water ligands followed by a trigonal compression of the hexaaqua ions in D_{3d} symmetry (Figure 1b,c). An "all-vertical" conformation of the planarly coordinated water ligands gives an a_{1g} orbital lower in energy than a pair of $e_g(D_{3d})$ orbitals, and further rotation of the water ligands 90° around the M–O bonds to an "all-horizontal" conformation still in D_{3d} symmetry reverses the energy order.[19,30] The "all-vertical" conformation was used in calculations for d^1 and d^6 ions, and the "all-horizontal" for d^2 ions, and resulted in significant energy gains for the largest ions.

Purpose of Present Work. Although only a few of the 4d metal ions have been established experimentally as hexahydrated ions in the +II (Ru, Cd) or +III (Mo, Ru, Rh, In) oxidation states, and then with low-spin ground states for the ruthenium and rhodium ions, we have performed theoretical calculations on the complete series of high-spin $[M(H_2O)_6]^{n+}$ (n = 2, 3) species. This allows a systematic discussion of how characteristic coordination properties (bond distances, ligand conformations, binding energies, symmetric stretching vibrational frequencies) are related to the occupation of the d orbitals and illustrates the influence of ligand field and Jahn–Teller effects in the two periods.

Previously, the experimental single-ion hydration enthalpies for 10 divalent ions of the first transition period were compared to the calculated binding energies of the hexahydrated complexes,[1a] followed by a study of the water-exchange rates based on a dissociative mechanism.[1b] For the second transition row, single-ion hydration enthalpies have been reported for five divalent (Sr, Tc, Pd, Ag, Cd) and five trivalent (Y, Nb, Mo, Rh, In) ions.[20] With the use of some well-characterized high-spin hexahydrated M^{2+} and M^{3+} ions as calibration points, the contributions of the calculated binding energy of the first solvation shell and energy contributions of further hydration layers (due to hydrogen bonding, polarization, etc.) to the hydration enthalpy are discussed in the present work in a similar way as before.[1-4] Furthermore, binding energies and M–O distances are compared on an equal basis for all hexahydrated di- and trivalent 3d and 4d elements, allowing a general discussion of the effects of the electronic structure on coordination and bonding and also of associative and dissociative water-exchange mechanisms for the di- and trivalent 3d ions in the following article.[31] The effects of low-spin states and changes in hydration numbers for some of the hydrated ions and the resulting deviations in structure (M–O distances) and energies (symmetric stretching vibration frequencies, hydration enthalpies) are also discussed and related to the electronic structure in the present work.

Methods

For all the hexaaqua clusters of the d-block ions, including the closed shell Ca^{2+}, Sr^{2+}, Ga^{3+}, and In^{3+} ions, the M–O distances have first been optimized in the highest possible symmetry, T_h. All systems have been studied at the SCF level of approximation, and in addition, some have been treated with CASSCF and CI methods, using the MOLECULE-SWEDEN program system.[32] The total binding energies, which correspond to a gas-phase reaction at 0 K, were obtained as the difference

$$\Delta E_b = E\{M(g)^{n+}\} + 6E\{H_2O(g)\} - E\{M(H_2O)_6(g)^{n+}\} \quad (1)$$

The planarly coordinated water molecules were kept with the gas-phase structure, as previously described.[1-3] The trigonal compression of

(29) Garmer, D. R.; Krauss, M. *J. Am. Chem. Soc.* **1992**, *114*, 6487.

(30) Cotton, F. A.; Kay Fair, C.; Lewis, G. E.; Mott, G. N.; Ross, F. K.; Schultz, A. J.; Williams, J. M. *J. Am. Chem. Soc.* **1984**, *106*, 5319.

(31) Åkesson, R.; Pettersson, L. G. M.; Sandström, M.; Wahlgren, U. *J. Am. Chem. Soc.*, following article in this issue.

(32) MOLECULE-SWEDEN is an electronic structure program written by J. Almlöf, C. W. Bauschlicher, M. R. A. Blomberg, D. P. Chong, A. Heiberg, S. R. Langhoff, P.-A. Malmqvist, A. P. Rendell, B. O. Roos, P. E. M. Siegbahn, and P. R. Taylor.

the "all-vertical" and "all-horizontal"" (Figure 1b,c) hexaaqua complexes in D_{3d} symmetry, still with the plane of the water ligands containing the M–O bond, was also investigated for d^1, d^6, and d^2 ions, respectively (medium-sized O/H basis, see below) by optimizing two parameters, R_6(M–O) and α. A regular octahedral MO_6 unit is obtained for α = 54.74° (half the tetrahedral angle).

For the 3d elements the same basis sets as those previously were used,[1-3] although for the trivalent ions additional s and p functions were left uncontracted in order to reduce the basis set superposition errors. The 4d metal ions have been described using the Hay and Wadt effective core potentials (ECP), which include relativistic effects.[33a] For the ions in the series Sr–Ag, small-core ECP's were used, where also the outer (4s, 4p) core orbitals are included in the valence shell. For Cd only a large-core ECP, where merely the 5s and 4d electrons are explicitly treated, was available.[33b] The results were calibrated against those of the small-core ECP by recomputing the $[Ag(H_2O)_6]^{3+}$ complex using the corresponding large-core ECP. The difference in the computed total binding energies obtained with the two ECP's for Ag was then used to relate the results for Cd to the other metal atoms in the series. The original metal basis sets were contracted to ⟨4s4p3d⟩ and ⟨2s2p2d⟩ in the small- and large-core ECP cases, respectively. For indium, no similar ECP description was available and this case was then treated at the all-electron level using a ⟨7s6p5d⟩ contraction of a (20s16p11d) primitive basis set optimized by Faegri.[34a] In this case, relativistic effects were included as a first-order perturbation theory estimate of the Darwin and mass–velocity terms. A calibration calculation on $[Ag(H_2O)_6]^{3+}$ with an equivalent all-electron basis set[34b] showed an acceptable consistency with the ECP results (5 kJ mol^{-1} lower binding energy), and no correction was applied to the indium results.

The contracted water basis set for the 4d elements was the medium-sized ⟨O:3s4p/H:2s⟩ previously used in similar studies.[1-3] This representation gives an artificially large dipole moment of the water ligands leading to an exaggerated binding energy in an $[M(H_2O)_6]^{n+}$ cluster.[3] For the divalent hexaaqua 3d ions, this effect was shown to give an almost constant contribution to the calculated binding energy along the series (190 ± 3 kJ mol^{-1}) but had little influence on the computed geometries.[1] Thus, the total binding energies of the divalent 4d ions, calculated with the medium-sized water basis, have been reduced by 190 kJ mol^{-1} in comparison with those of the dipositive 3d complexes, computed with a large water basis set. For the tripositive 3d ions, a similar recalculation at the optimized geometry using the larger water basis set (including two oxygen d and one hydrogen p functions), as described in the previous study on the corresponding divalent complexes,[1a] lowered the total binding energy by 241 ± 3 kJ mol^{-1} in the series. This basis set correction was then applied to the trivalent 4d complexes to make their binding energies comparable with those of the 3d elements. For the larger basis set, a modified version of the direct SCF program DISCO,[35] running on a Cray X-MP/416, was used.

Comparisons of computed binding energies and M–O distances between the first and second transition periods require equivalency between the all-electron (AE) and ECP metal basis sets, respectively. As a test, the $[Mn(H_2O)_6]^{2+}$ system was reoptimized using both the metal ion AE and ECP basis sets in a way similar to that for Ag^{3+} (see above). The medium-sized water basis yielded an Mn–O distance of 2.227 Å and a binding energy of 1384 kJ mol^{-1}, only slightly different from the corresponding values in the all-electron case (2.233 Å, 1369 kJ mol^{-1}), and also a similar charge of the manganese ion (ECP, +1.68; AE, +1.73). Thus, it seems that the approximations associated with the ECP are small enough (≤1.5% of the total binding energy) to allow direct comparisons between the two periods.

At the SCF level of approximation, the exchange stabilization in high-spin artificially favors the high-spin over the low-spin states. In order to make comparisons of different spin states some additional calculations were performed at the multireference CI level with all d valence orbitals correlated and with the Davidson correction introduced to account for size inconsistencies. The reference space consisted of all configurations with coefficients greater than 0.05 from a CASSCF calculation with all d orbitals active. The correlation treatment was improved by extending the metal basis sets with an additional f function with exponents from a three-term fit to an STO function. The systems chosen for this treatment were the hexahydrated clusters of Fe^{2+}, Co^{3+}, Ru^{2+}, Rh^{3+} (d^6), Ru^{3+} (d^5), Cr^{2+} (d^4), and the square-planar tetrahydrates of Ni^{2+} and Pd^{2+} (d^8).

Finally, for d^2 and high-spin d^7 ions, a two-determinant description is necessary in order to describe the atomic ground state in the ligand field, as described previously.[1] Thus, in order to obtain a comparable SCF level binding energy, a correction ΔE_{CAS} obtained by CASSCF calculations with the 3d (or 4d) electrons in the active space was added. The values calculated are, in T_h symmetry, Ti^{2+} 16.34, Co^{2+} 30.01, V^{3+} 17.69, Ni^{3+} 29.63, Zr^{2+} 7.59, Rh^{2+} 18.7, Nb^{3+} 7.90, and Pd^{3+} 13.85 kJ mol^{-1} and, in D_{3h} symmetry, Ti^{2+} 8.96, V^{3+} 5.78, Zr^{2+} 4.36, and Nb^{3+} 3.22 kJ mol^{-1}.

Results and Discussion

I. Metal–Oxygen Distances. The calculated M–O distances for the high-spin di- and trivalent complexes in T_h symmetry are given in Table 1 and plotted in Figure 2. The dashed curves connecting the ions without additional ligand field stabilization due to the splitting of the d orbitals, i.e. the d^0, d^5, and d^{10} ions, decrease smoothly with increasing nuclear charge. For the intermediate ions the M–O distances are shorter than expected from the connecting curves, with minima for the d^3 and d^8 electron configurations which have the largest ligand field stabilization energies. Comparisons are made in Figure 2 with M–O distances from two series of isomorphous crystal structures, the ammonium Tutton and the cesium alum salts, for di- and trivalent 3d ions, respectively.[5,7b] The high-precision experimental values are, as previously,[1] found to be somewhat shorter than those calculated (Table 1). The deviations are, however, larger than would be expected from insufficient corrections for, for example, electron correlation and relativistic effects, which both should act to shorten the calculated M–O bond lengths. One plausible reason is that the hydrogen bonds to a second coordination sphere in condensed phases polarize the water molecules and shorten the M–O bonds, as compared to those in the isolated cluster in the calculations.[39] Another is the systematic corrections required to make the crystal structure values comparable to the quantum chemical (0 K) equilibrium distances. The distance obtained from the mean positions of a pair of atoms in a crystal is usually shorter than the actual average bond length between the instantaneous positions of the atoms. Moreover, the observed distances tend to decrease with increasing temperature, and the shortening may amount to 0.03 Å or more.[41] Tilting of the water ligand by the directed hydrogen bonds in a lattice would be expected to increase the M–O bond length (cf. Tables 1 and 4 in ref 3).[39b] However, in comparisons of homologous series, such effects should be constant or vary in a similar way, as evidently is the case in Figure 2.

The mean M–O distances from the structures for the ammonium Tutton salts with M = V^{2+}, Cr^{2+}, Mn^{2+}, Fe^{2+}, Co^{2+}, Ni^{2+}, Cu^{2+}, and Zn^{2+} [7b] show a trend very similar to that of our calculated values (Figure 2a). In the same work also the crystal structures of an isomorphous series of $[M(H_2O)_6]SiF_6$ salts were determined for the same metal ions, but this gave significantly shorter M–O bonds for most ions. Evidently, the more symmetric and rigid surroundings of the hexaaqua ions in the hexafluorosilicate salts partly reduces the ligand field induced variations of the M–O bond lengths and even causes complete suppression of

(33) (a) Hay, P. J.; Wadt, W. R. *J. Chem. Phys.* **1985**, *82*, 299. (b) *Ibid.* 270.

(34) (a) Faegri, K., Jr. Private communication. (b) Faegri, K., Jr.; Biran, G. Theoretical Chemistry Technical Note, University of Oslo, November 1987.

(35) (a) Almlöf, J.; Faegri, K., Jr.; Forsell, K. *J. Comput. Chem.* **1982**, *3*, 385. (b) Saebø, S.; Almlöf, J. *Chem. Phys. Lett.* **1987**, *154*, 521.

(36) (a) Einspahr, H.; Bugg, C. E. *Acta Crystallogr., Sect. B* **1980**, *36*, 264. (b) Carugo, O.; Djinovic, K.; Rizzi, M. *J. Chem. Soc., Dalton Trans.* **1993**, 2127.

(37) Brooker, M. H. In *The Chemical Physics of Solvation*; Dogonadze, R. R.; Kálmán, E., Kornyshev, A. A., Ulstrup, J., Eds.; Elsevier: Amsterdam, 1986; Part B, Chapter 4.

(38) Johansson, G.; Sandström, M. *Acta Chem. Scand.* **1987**, *A41*, 113.

(39) (a) Chiari, G.; Ferraris, G. *Acta Crystallogr., Sect. B* **1982**, *38*, 2331. (b) Friedman, H. L.; Lewis, L. *J. Solution Chem.* **1976**, *5*, 445.

(40) Tachikawa, H.; Ichikawa, T.; Yoshida, H. *J. Am. Chem. Soc.* **1990**, *112*, 977, 982.

(41) Trueblood, K. N. In *Accurate Molecular Structures*; IUCr Monographs on Crystallography, No. 1.; Domenicano, A., Hargittai, I., Eds.; Oxford University Press: Oxford, U.K., 1992; Chapter 8.

Table 1. Metal–Oxygen Distances, R_6(M–O)/Å, and Raman Symmetrical Stretching Frequencies, $\tilde{\nu}_1(A_g)$/cm^{-1}, of Hydrated 3d and 4d Ions (Calculated Values for $[M(H_2O)_6]^{n+}$ Complexes in T_h Symmetry)

	divalent ions				trivalent ions			
M	R_{exptl}(M–O)	R_6(M–O)	$\tilde{\nu}_{exptl}$	$\tilde{\nu}_{calcd}$	R_{exptl}(M–O)	R_6(M–O)	$\tilde{\nu}_{exptl}$	$\tilde{\nu}_{calcd}$
Ca	2.39[a,b]	2.399	~290[c]	273				
Sc		2.307		308	2.07[d,e]	2.167	440[e]	416
Ti		2.252		303	2.028[f]	2.110	517[g]	427
V	2.128[h]	2.201		317	1.992[f]	2.063	525[g]	447
Cr	2.167[h,i]	2.225[i]	~455[j]	318[k]	1.959[f]	2.025	540[g,i]	460
Mn	2.175[h]	2.233	358[c]	311 (310)[m]	1.991[f,n]	2.042[i]		447[k]
Fe	2.126[h]	2.185	380[c]	328	1.995[o]	2.052 (2.062[m])	506[g]	446 (451[m])
Co	2.092[h]	2.143	375[p]	338		2.017		465
Co[q]					1.873[f]	1.933	548[p]	484
Ni	2.056[h]	2.108	390[c]	341		1.986		474
Cu	2.085[h,i]	2.121[i]	436[o]	345[k]		1.954		489
Zn	2.092[h]	2.123	390[c]	344		1.972		451
Ga					1.944[f]	1.987	537[g]	464
Sr	2.57[a,r]	2.581		242				
Y		2.489		305	2.29[a,s]	2.354	380[t]	359
Zr		2.413		309		2.286		378
Nb		2.350		318		2.231		406
Mo		2.399		331	2.089[u]	2.180		430
Tc		2.440		303		2.208		444
Ru		2.378		326		2.246		412
Ru[q]	2.12[v]	2.197	424[v]	393	2.014[w]	2.090	532[v]	470
Rh		2.331		315		2.199		416
Rh[q]					2.016[g]	2.055	548[x]	499
Pd		2.276		327		2.160		439
Ag		2.306[i]		317		2.127 (2.149[x])		460 (434[y])
Cd	2.285[z]	2.308	356[c]	322		2.147		387
In					2.112[f]	2.183	475[c]	417

[a] Estimated for the hydration number $n = 6$ and $R(H_2O) = 1.39$ Å, refs 16 and 36. [b] Solution value 2.42 Å ($n > 6$), ref 16. [c] Solution value, ref 14b. [d] Estimated for $n = 6$ from alum salt, ref 5a. [e] Solution value 2.18 Å ($n \approx 7$), ref 14. [f] Alum salt, ref 5a (Cr–O 1.961 Å, neutron diffraction, ref 12c). [g] Alum salt, ref 13b. [h] Tutton salt, mean M–O value, ref 7b. [i] Mean value of Jahn–Teller distorted geometry. [j] Reference 1b. [k] Calculated for T_h symmetry. [l] Alum salt, solution value 522 cm^{-1}, ref 13c. [m] Optimized with the large O/H basis set. [n] Suppressed Jahn–Teller distortion. [o] Alum salt, ref 12b (1.994 Å, neutron diffraction). [p] Reference 37. [q] Low spin. [r] Solution value ($n \approx 8$) 2.64 Å, ref 16. [s] Solution value ($n \approx 8$) 2.37 Å, ref 17. [t] Solution value ($n \approx 8$), ref 14. [u] Alum salt, ref 19 (2.089 Å, neutron diffraction, ref 5b). [v] References 9 and 10. [w] Alum salt, ref 12a (2.010 Å, neutron diffraction, ref 5b). [x] Alum salt, solution value 529 cm^{-1}, ref 13c. [y] All-electron SCF + relativistic correction. [z] Reference 38, corrected for thermal "riding" motion.

the Jahn–Teller distortions for Cr^{2+} (see Jahn–Teller Effects in Hexaaqua Ions) and to some extent also for Cu^{2+} by opposing an expansion of the lattice to accommodate the larger $[M(H_2O)_6]^{2+}$ ions.

A similar comparison has been made for the hexahydrated trivalent 3d ions on the basis of the cesium alum structures containing Sc^{3+}, Ti^{3+}, V^{3+}, Cr^{3+}, Mn^{3+}, Fe^{3+}, Co^{3+}, and Ga^{3+} (Figure 2b).[5] Again the curves describing the variations in the experimental and the theoretical M–O bond lengths have similar shapes with a decreasing difference to the right in the row. The Co^{3+} ion breaks the trend, however, because of its low-spin ground state. An extrapolation of the experimental curve shows the Co–O bond to be ca. 0.08 Å shorter than the expected high-spin value, similar to the calculated difference 0.084 Å (cf. Table 1).

The regular (nearly linear) decrease of the experimental M–O distances found for the ions Ti^{3+}, V^{3+}, Cr^{3+}, and low-spin Co^{3+}, with an increasing number of d electrons occupying the $t_{2g}(O_h)$ orbitals, is discussed in ref 5b. Similar decreases occur prior to the minima in the theoretical curves in Figure 2 for all series of di- and trivalent 3d and 4d high-spin hexahydrated ions. The steeper slopes and deeper minima for the M–O distances of the second-row (4d) elements are in keeping with the more pronounced influence of the ligand field effect on the spatially more extended 4d orbitals. There are few experimental data to compare with for these elements,[5b] mainly due to the frequent occurrence of low-spin states and metal-metal bonding but also because of the size of the hydrated ions, which for the early transition elements often is large enough to allow more than six water molecules to be coordinated in solution. This would certainly be the case for most of the divalent early 4d transition metal ions, as shown by a comparison of their calculated bond lengths with those of Sr^{2+} and Ca^{2+} in the first period[16,36] (Table 1). Increased coordination numbers in solution occur at a smaller size of the trivalent ions because of their higher charge, with about eight water molecules around Y^{3+},[17] and also with Sc^{3+} in the first transition row large enough to accommodate probably seven water ligands.[14]

II. Alternative Conformations of Hexahydrated Ions. The splitting of the three degenerate orbitals of $t_g(T_h)$ symmetry into an $e_g(D_{3d})$ pair and one a_{1g} orbital was investigated by test calculations on $[Mn(H_2O)_6]^{2+}$, which has all 3d orbitals singly occupied, allowing direct comparisons of their energies. The two different $T_h \rightarrow D_{3d}$ conversions, to the "all-vertical" and the "all-horizontal" D_{3d} conformations, which both may proceed by a 45° rotation (in opposite directions) of the water molecules around the M–O bonds, were studied. The orbital energies confirmed that the $a_{1g}(D_{3d})$ orbital (almost pure Mn $3d_{z^2}$, note the change of the z direction in Figure 1b,c) is stabilized in the "all-vertical" conformation and destabilized relative to the $e_g(D_{3d})$ in the "all-horizontal" conformation, as proposed previously.[19,30] The orbital splitting becomes more pronounced by a trigonal compression of the MO_6 unit, which also should favor a $3d_{z^2}$–4s mixing. For $[Mn(H_2O)_6]^{2+}$ the total energy of the "all-vertical" D_{3d} conformation was thus clearly higher than that of the T_h (22.4 kJ mol^{-1} at an optimized angle $\alpha = 56.0°$), with indications of an even slightly higher energy for the "all-horizontal" D_{3d} conformation. The energy of the $e_g(T_h)$ orbitals is not affected by the rotation of the water molecules, and the energy increase is rather due to the increased repulsion between the protons and the larger Pauli repulsion against the occupied oxygen orbitals as shown by the increasing antibonding overlap.

The "all-vertical" conformation in which the $a_{1g}(D_{3d})$ orbital is stabilized was used for calculations on the d^1 ions Sc^{2+}, Ti^{3+}, Y^{2+}, and Zr^{3+} and the high-spin d^6 ions Fe^{2+}, Ru^{2+}, and Rh^{3+}, and the "all-horizontal", for the d^2 ions Ti^{2+}, V^{3+}, Zr^{2+}, and Nb^{3+}. All d^1 ions, except the smallest, i.e., Ti^{3+}, showed lower energy in the "all-vertical" D_{3d} conformation than in T_h (Table 2). The

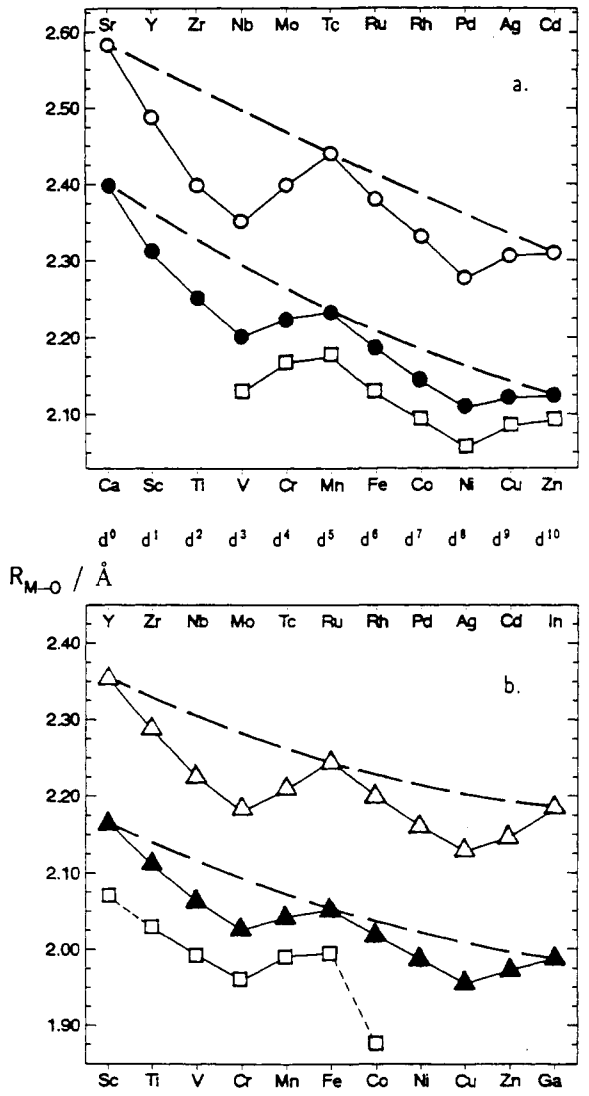

Figure 2. Calculated M–O distances of d-block high-spin $[M(H_2O)_6]^{n+}$ complexes in T_h or D_{3h} symmetry for increasing numbers of d electrons: (a) divalent 3d (filled circles) and 4d (open circles) metal ions. The squares correspond to Tutton salts;[7] (b) trivalent 3d (filled triangles) and 4d (open triangles) metal ions, compared with cesium alum salts (squares), with Co^{3+} in low-spin[6] and Sc^{3+} estimated from unit cell dimensions.[5] The reference lines (long dashes) connect d^0, d^5, and d^{10} ions without additional ligand field stabilization due to the splitting of the d-orbital energy levels.

optimized metal–oxygen distances were close to the T_h values, cf. Table 1, but the α angles show a slight trigonal compression of the central MO_6 octahedral unit. The amount of the distortion and the preference for this type of D_{3d} structure are connected to the radius of the cluster, which makes the increased proton–proton repulsion in the D_{3d} structure less important for the larger ions. Also the occupation of the d orbitals for the Fe^{2+}, Ru^{2+}, and Rh^{3+} ions (high spin d^6 with the $a_{1g}(D_{3d})$ orbital doubly occupied) counteracts the distortion of the MO_6 octahedron. The lowering of the $a_{1g}(D_{3d})$ orbital energy does not outweigh the higher repulsion between the protons for the small Fe^{2+} ion, but Ru^{2+} and Rh^{3+} are marginally more stable in the D_{3d} than in the T_h symmetry (Table 2).

Even though these trends are clear, the energy differences between the conformations are small and, for example, hydrogen bonding and differences in O–H distances in condensed phases may well give different results than this gas-phase comparison with fixed water geometry. Thus, ESR and electron spin echo studies of the $[Ti(D_2O)_6]^{3+}$ ion in an amorphous 2-propanol/D_2O glass support an "all-vertical" D_{3d} structure.[40] Also,

Table 2. Alternative Structures of Hexaaqua Complexes for d^1 and d^6 Ions "All-Vertical" and for d^2 Ions "All-Horizontal" Conformations in D_{3d} Symmetry

M	d^n	R_6(M–O)/Å	α^a	q(M)[b]	δE^c/kJ mol^{-1}
		Vertical Trigonal-Planar H_2O			
Sc^{2+}	$3d^1$	2.309	57.89	+1.86	−7.4
Ti^{3+}	$3d^1$	2.110	56.27	+2.36	+3.5
Fe^{2+}	$3d^6$	2.185[d]	56.72	+1.62	+10.9
Y^{2+}	$4d^1$	2.486	63.90	+1.73	−50.7
Zr^{3+}	$4d^1$	2.286[d]	57.89	+2.37	−20.9
Ru^{2+}	$4d^6$	2.378[d]	57.43	+1.80	−0.9
Rh^{3+}	$4d^6$	2.199[d]	56.52	+2.20	−1.1
		Horizontal Trigonal-Planar H_2O			
Ti^{2+}	$3d^2$	2.253	56.74	+1.79	−4.4[e]
V^{3+}	$3d^2$	2.067	56.25	+2.24	+5.8[e]
Zr^{2+}	$4d^2$	2.399	55.78	+1.75	−16.0[e]
Nb^{3+}	$4d^2$	2.224	55.58	+2.40	−8.3[e]
		Horizontal Tilted (Lone-Pair) H_2O			
Ti^{2+}	$3d^2$	2.252[d]	53.12	+1.45	~+150
V^{3+}	$3d^2$	2.063[d]	54.74[f]	+1.82	~+200

[a] Angle between the C_3 axis and the M–O bond, see Figure 1b,c. [b] Metal atom charge from Mulliken population analysis. [c] $\delta E = \Delta E_b(T_h) - \Delta E_b(D_{3d})$. [d] Not optimized. [e] Calculated using $\Delta E_{CAS}(D_{3d})$ corrections, see Methods. [f] Fixed at one-half of the tetrahedral angle.

theoretical calculations on the MR-SDCI level on an isolated $[Ti(H_2O)_6]^{3+}$ cluster were reported to give the lowest energy for "all-vertical" D_{3d} symmetry. However, the comparisons were not made with the cluster in T_h symmetry but rather with a D_{2h} structure with all four equatorial water molecules perpendicular to the xy plane, giving a more unfavorable proton–proton repulsion. This is also shown by the energy gain obtained when allowing a Jahn–Teller distortion of this structure,[40] which is much higher than those caused by degenerate t_g orbitals in T_h structures (see Jahn–Teller Effects in Hexaaqua Ions).[29] Calculations on $[Sc(H_2O)_6]^{2+}$ using both the medium and the large O/H basis sets verified that the energy differences between the different conformations were not basis-set dependent.

The "all-vertical" D_{3d} conformation was in all cases more favorable for the $4d^1$ and high-spin $4d^6$ ions than for the corresponding 3d ions, as expected from the increase in ligand field effects and the larger size of the 4d complexes. The energy gain as compared to the T_h symmetry was most pronounced for $[Y(H_2O)_6]^{2+}$ (50.7 kJ mol^{-1}), and the α value (63.9°) shows that considerable distortion from an octahedral MO_6 core is favorable for this large d^1 ion (Table 2).

The "all-horizontal" D_{3d} conformation was found to be 16.0 and 8.3 kJ mol^{-1} more stable than the T_h for the $4d^2$ ions Zr^{2+} and Nb^{3+}, respectively. In applying the center of gravity principle for the $t_g(T_h)$ orbitals, i.e. the perturbation of $\pm\delta\epsilon$ for the e_g orbital corresponds to $\mp 2\delta\epsilon$ for a_{1g}, in a comparison between the two D_{3d} geometries, one would expect energy gains similar to those for the neighboring $4d^1$ ions, Zr^{3+} and Y^{2+}. However, the larger size of the $4d^1$ complexes allows larger trigonal compression, as seen from the α values, and thus higher energy stabilization. For the $3d^2$ ion Ti^{2+}, the "all-horizontal" D_{3d} conformation is slightly favored, but for the small V^{3+}, the T_h symmetry is still lower in energy (Table 2), and by analogy with the d^6 ions, this is also expected for all of the d^7 ions.

The $[V(H_2O)_6]^{3+}$ complex in the solid compound $[V(H_2O)_6][H_5O_2](CF_3SO_3)_4$ is close to a D_{3d} conformation with nearly "all-horizontal" flat water molecules.[30] However, this conformation is influenced by the directed hydrogen bonding in the solid state, an effect which is not present in the theoretical study. This argument also applies to the "tilt" of the water ligands observed, for example, for the Tutton salts.[7b,c] For two $3d^2$ ions, Ti^{2+} and V^{3+}, the calculations showed that "tilting" of the water molecules toward a pyramidal "lone-pair" coordination of the oxygen atom raises the energy considerably for an isolated hexaaqua cluster. The weakened ion–dipole attraction seems,

Table 3. Low-Spin Hexaaqua Complexes for d^4 (Cr^{2+}), d^5 (Ru^{3+}), and d^6 Ions and Energy Comparisons with High-Spin States at Different Levels of Computation

M	R(M–O)/Å[a]	δE-(SCF)[b,c]	δE-(DISCO)[b,d]	δE-(CAS)[b,e]	δE-(CI)[b,f]
Cr^{2+}	2.152[g]	194.4		164.9	146.5 (108)[h]
Fe^{2+}	2.071	328.9	334.8	277	204 (164)[h]
Co^{3+}	1.933	255.5	259.0	207	43.4
Ru^{2+}	2.197	73.3		45.8	14.5
Ru^{3+}	2.090	109.6		79.2	47.5
Rh^{3+}	2.055	−79.8		−102.5	−254.5

[a] Low-spin M–O distance optimized at SCF level. [b] $\delta E = E_{\text{low-spin}} - E_{\text{high-spin}}$/kJ mol^{-1}. [c] Single-configuration SCF, medium O/H basis. [d] SCF, large O/H basis. [e] All 3d (4d) orbitals active. [f] MRCI + Davidson correction, medium O/H basis, metal basis set extended with one f function, 3d (4d) orbitals correlated. [g] 2.155 Å when optimized at the MRCI level. [h] Including an experimentally based correction for the atomic high-/low-spin state separation, see Low-Spin States.

however, to be partly compensated for by an increased covalencyin the M–O bond as indicated by the lower metal charge, see Table 2.

III. Jahn–Teller Effects in Hexaaqua Ions. Silver(II), with the electron configuration $4d^9$, would be expected to exhibit first-order Jahn–Teller distortions in a hexaaqua ion in a way similar to $[Cu(H_2O)_6]^{2+}$.[2,3] In textbooks, however, Ag^{2+} ions in aqueous solution are proposed to have a transient existence as $[Ag(H_2O)_4]^{2+}$ complexes with a square-planar structure.[42] In contrast to the case for Cu^{2+}, the disproportionation $2Ag^+ \rightleftharpoons Ag(s) + Ag^{2+}$ has a very low equilibrium constant ($K \approx 10^{-20}$ M^{-1}),[42] proposed to be a result of the low hydration enthalpy of Ag^{2+}.

The Jahn–Teller effect on $[Ag(H_2O)_6]^{2+}$ was studied in a way similar to that previously for Cu^{2+},[2,3] i.e. with optimizations of an axial (R_{ax}) and an equatorial (R_{eq}) M–O distance in D_{2h} symmetry corresponding to a tetragonal distortion of the T_h structure. The results were qualitatively similar to those for the 3d ions, with the elongated octahedral Ag–O coordination ($2R_{ax}$ = 2.486, $4R_{eq}$ = 2.223 Å) slightly more stable (2β = 101 cm^{-1}) than the compressed structure ($2R_{ax}$ = 2.172, $4R_{eq}$ = 2.373 Å). The Jahn–Teller energy (E_{JT}, i.e. the energy difference from the optimized regular T_h structure) was 1203 cm^{-1} (14.4 kJ mol^{-1}), which is twice as large as that for Cu^{2+} (582 cm^{-1}).[1] The geometric distortion, as given by the Jahn–Teller radius, $R_{JT} = [\sum(r-\bar{r})^2]^{1/2}$, is also larger, 0.30 Å (0.24 Å for $[Cu(H_2O)_6]^{2+}$).[3] Despite the rather large differences between the Ag–O distances in the elongated and the compressed structures, the mean value is close to that in regular T_h symmetry, as previously found for similar Jahn–Teller distortions.[3] Considering the difference in size, the Ag^{2+} ion does not seem to have an anomalously lower hydration enthalpy than that of Cu^{2+} (cf. also Zn^{2+} and Cd^{2+}, Table 3), and the similarity of the results is consistent with a tetragonally elongated octahedral hexaaqua complex as for Cu^{2+}, rather than a four-coordinated square-planar complex.

The irregular variations of the M–O bond lengths found in the solid state for Jahn–Teller distorted complexes,[7,27] not only for the axial but also for the equatorial distances, show that the lattice and packing forces can completely supercede the relatively small energies gained from the Jahn–Teller distortions. Also, the efficiency with which the hydrogen bonds can be formed was found to induce significant variations in metal–water bond length and conformation (except for V^{2+}).[7b-d] Comparisons with crystal structure values are therefore of uncertain value as a measure of such electronically induced effects, as is evident from, for example, the complete suppression of Jahn–Teller distortions for hydrated Cr^{2+}, Cu^{2+}, and Mn^{3+} ions in high site-symmetries.[5,7a,b]

The hexaaquachromium(II) ion shows no Jahn–Teller distortion in the colorless $[Cr(H_2O)_6]SiF_6$ salt and also has an anomalously short Cr–O distance, 2.106(2) Å, i.e. 0.06 Å shorter than the mean value (2.167 Å) of the distorted complex in the blue $(NH_4)_2[Cr(H_2O)_6](SO_4)_2$ Tutton salt.[7b] The compression of the hexaaquametal ions noted in the comparison between the hexafluorosilicate salts as compared to the corresponding Tutton salts (except for V^{2+}) is more pronounced for Cr^{2+} than for any of the other ions in this study.[7] As a result of the short Cr–O distances in the $[Cr(H_2O)_6]SiF_6$ salt, the ligand field splitting of the d orbitals should increase and make a low-spin structure more favorable. We have therefore optimized the Cr–O distances in T_h symmetry for both low- and high-spin states. Electron correlation effects are more important for the total energy in low-spin states as discussed later (see Low-Spin States), and MRCI methods with all d electrons correlated were used for the optimizations. We find that the energy curve for the low-spin state crosses over the high-spin curve at 1.92 Å. Even though the energy at the minimum of the low-spin curve still is 147 kJ mol^{-1} higher than the high-spin energy, other comparisons in Table 4 show that the calculated energy differences on isolated clusters are not of good predictive value for high → low spin transitions. An important factor for the stabilization of the smaller low-spin complex is probably the influence of the more strongly coordinated second sphere, which may shift the relative positions of the curves. It is noteworthy, however, that the calculated difference in the equilibrium Cr–O bond lengths between the high- and low-spin states is 0.07 Å, close to the experimental difference of 0.06 Å. We thus conclude that the experimental observations are consistent with a low-spin state of the Cr^{2+} ion in the rigid high-symmetry crystal lattice of the $[Cr(H_2O)_6]SiF_6$ salt, but other experimental methods (e.g. UV–vis and ESR spectra) should be used to confirm this proposal.

The minor Jahn–Teller effect expected from the splitting of degenerate t_g (T_h) orbitals by lowering the symmetry[29] was checked by an optimization of $[Fe(H_2O)_6]^{2+}$ in the D_{2h} symmetry and

Table 4. Theoretical Binding Energies, ΔE_b[a], of the Hexahydrated 3d and 4d Ions in High-Spin (Large O/H Basis) and Single-Ion Hydration Enthalpies, $\Delta H°_{hyd}$[b]

	divalent ions		trivalent ions	
M	ΔE_b	$-\Delta H°_{hyd}$	ΔE_b	$-\Delta H°_{hyd}$
Ca	1002	1577(6)		
Sc	1097[c]		2170	3897(10)
Ti	1153[c,d]	1862(15)	2322	4154(20)
V	1225	1918(15)	2432[d]	4375(20)
Cr	1208[e]	1904(6)	2567	4560(20)
Mn	1179	1841(6)	2553[e]	4544(30)
Fe	1245	1946(6)	2498	4430(10)
Co	1287[d]	1996(6)	2615	4651(20)[f]
Ni	1350	2105(6)	2702[d]	
Cu	1344[e]	2100(6)	2819	
Zn	1334	2046(6)	2814	
Ga			2780	4700(10)
Sr	859	1443(6)		
Y	1012[c]		1818	3583(10)
Zr	1047[c,d]		2006[e]	
Nb	1128		2126[c,d]	4195(20)
Mo	1041		2274	4290(20)
Tc	987	1858(25)	2175	
Ru	1060[e]		2082	
Rh	1110[d]		2216[e]	4495(20)[f]
Pd	1189	1989(20)[g]	2308[d]	
Ag	1155,[e] 1150[h]	1931(20)	2459,[e] 2481[i]	
Cd	1138	1807(6)	2476, 2454[j,k]	
In			2281[h]	4112(10)

[a] The ΔE_b/kJ mol^{-1} values (eq 1) include basis set corrections −190 and −241 kJ mol^{-1}, respectively, for the di- and trivalent 4d ions (Sr–In), see text. [b] Reference 20. [c] D_{3d} symmetry, see text and Table 2. [d] Calculated using ΔE_{CAS} corrections, see Methods. [e] Tetragonally elongated Jahn–Teller distorted geometry. [f] Low spin. [g] 4-coordinated square-planar structure. [h] All-electron SCF + relativistic correction. [i] Small core ECP. [j] Large-core ECP, 36 core electrons, (2s,2p,3d) valence basis set. [k] Corrected for difference between large and small core ECP, +17 kJ mol^{-1}.

(42) Cotton, F. A.; Wilkinson, G. *Advanced Inorganic Chemistry*, 5th ed.; Wiley Interscience: New York, 1988; Chapter 19-I-3,4.

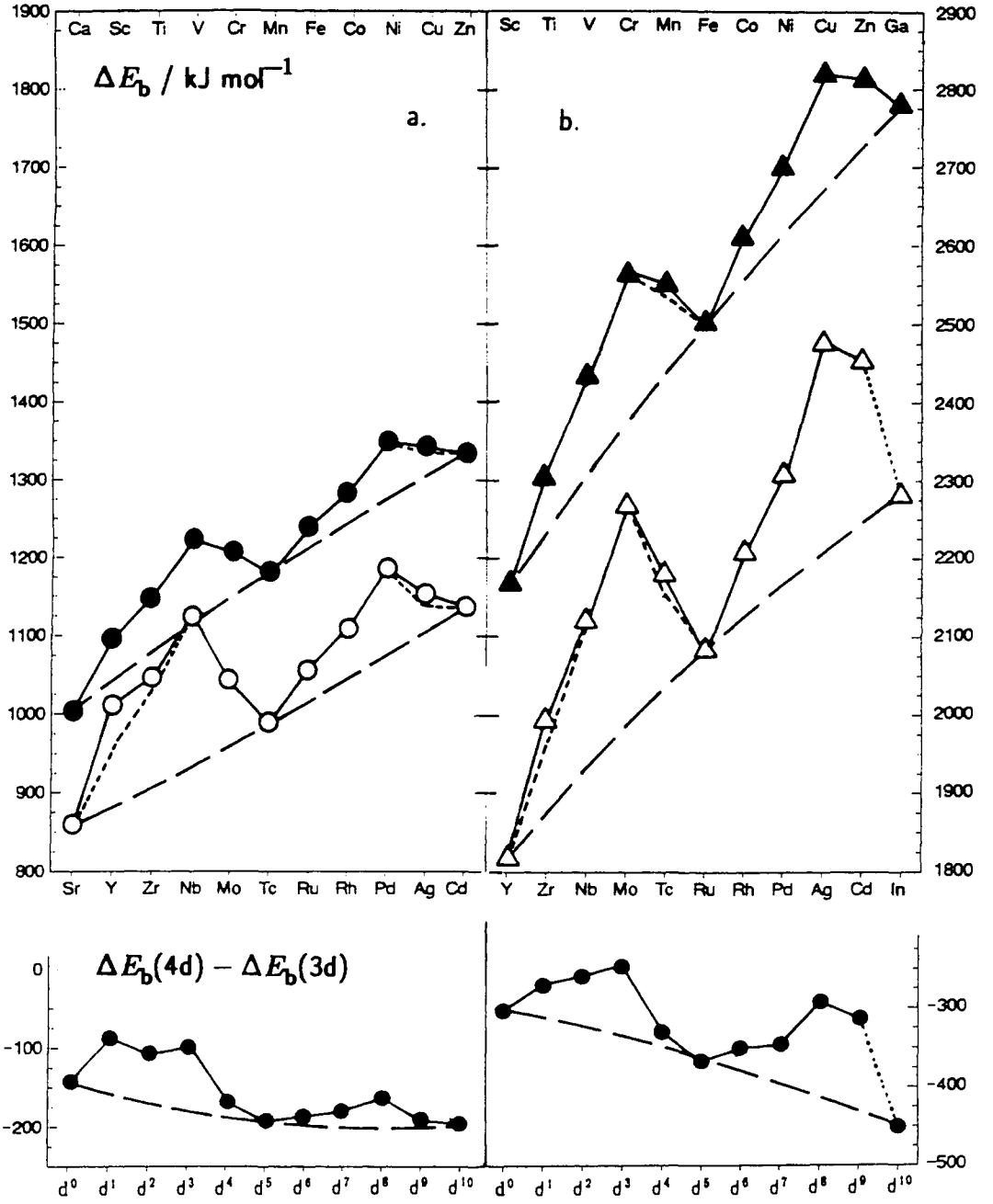

Figure 3. Theoretical binding energies, ΔE_b/kJ mol^{-1}, for high-spin hexaaqua complexes of the (a) divalent ions and (b) trivalent ions of the 3d (filled symbols) and 4d (open symbols) elements, respectively, with the difference (4d – 3d) below (circles). The reference lines (long dashes) connect d^0, d^5, and d^{10} ions. Calculated energy gains in D_{3d} (Sc^{2+}, 7; Ti^{2+}, 4; Y^{2+}, 51; Zr^{2+}, 16; Nb^{3+}, 8; Zr^{3+}, 21 kJ mol^{-1}) and D_{2h} (Cr^{2+}, 11; Cu^{2+}, 7; Ag^{2+}, 14; Mn^{3+}, 14 kJ mol^{-1}; elongated Jahn–Teller) symmetry are indicated by the line (short dashes) corresponding to T_h symmetry (Tables 2 and 4). The In^{3+} and to some extent the Ga^{3+} values are more uncertain due to differences in basis sets (see text).

resulted in a slightly compressed structure ($2R_{ax}$ = 2.158, $4R_{eq}$ = 2.201 Å) but an insignificant energy gain, E_{JT} = 44 cm^{-1} (0.5 kJ mol^{-1}).

IV. Binding Energies in High-Spin Hexahydrates. The binding energies ΔE_b of the high-spin $[M(H_2O)_6]^{n+}$ (n = 2, 3) clusters in T_h symmetry (D_{2h} for the tetragonally elongated Jahn–Teller systems, Cu^{2+}, Cr^{2+}, Mn^{3+}, and Ag^{2+}) are given in Table 4. Comparisons are made between the divalent 3d and 4d ions in Figure 3a and between the trivalent ions in Figure 3b, where also the additional energy gains from the D_{3d} conformations (Table 2) and Jahn–Teller effects are shown and display the expected double-humped features for an octahedral ligand field with maxima for the d^3 and d^8 metal ions.[5] The 4d ions have lower overall binding energies than the 3d for the same electron configuration in the outer d shell but a higher energy gain from the larger splitting of the 4d orbitals in the ligand field. The lower total energies are a result of the larger ion size, as can be seen from the plots of ΔE_b (high-spin) versus $1/R_6$(M–O) in Figure 4. The displacement of the fitted lines for the 4d ions relative to the 3d shows, however, that the bonds are stronger for the same ion size, consistent with the higher charge transfer and more covalent bonding evident from the Mulliken population analyses (Table 6). The almost linear energy correlations against $1/R_6$(M–O) indicate that electrostatic interactions dominate the bonding (an $1/R^2$ dependence would be expected for a pure ion–dipole interaction,[43] but the insensitivity is shown by the plot of ΔE_b *vs* R_6 in ref 1a). Ions with slightly higher binding energies than expected from the correlation are Y^{2+} and Nb^{2+} in D_{3d} symmetry and Cd^{3+}, Ga^{3+}, and Zn^{3+} with high covalency.

In addition, the CI energy values from Table 3 are plotted in

(43) Bockris, J. O'M.; Reddy, A. K. N. *Modern Electrochemistry*; Plenum: New York, 1970; Vol. 1, Chapter 2.

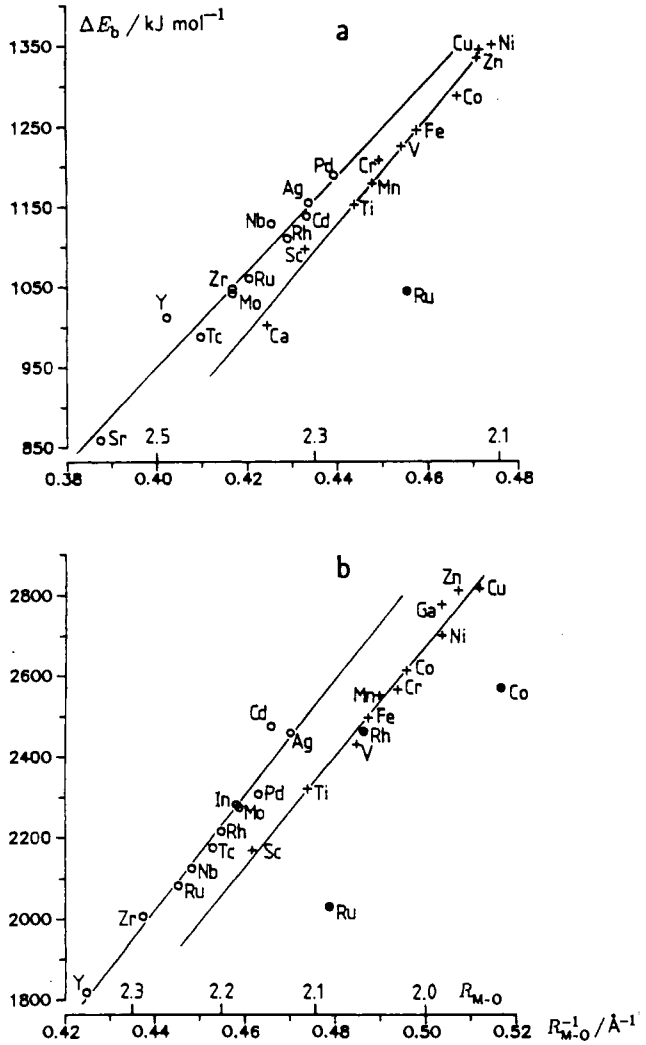

Figure 4. Theoretical binding energies, ΔE_b, for high-spin hexaaqua complexes of the (a) divalent ions and (b) trivalent ions of the 3d (crosses) and 4d (open circles) elements, respectively, plotted as a function of R_6^{-1}/Å^{-1}. Low-spin ions (MRCI values) are shown by filled circles.

Figure 4 for the low-spin hexahydrated ions Ru^{2+}, Ru^{3+}, Rh^{3+}, and Co^{3+} and show the expected contraction for a comparable binding energy also for Rh^{3+}. The contraction is even larger for the low-spin 4-coordinated square-planar Pd^{2+} and Ag^{3+} ions (Table 7).

The more pronounced energy gains from the stronger ligand field effects for the 4d ions, despite their lower total binding energies, are evident from Figure 3. All 4d – 3d energy differences lie above the connecting curves through the nonstabilized ions with 0, 5, and 10 d-electrons, and in particular, the $4d^3$ metal ions (Mo^{3+} and Nb^{2+}) are favored over their $3d^3$ counterparts (Cr^{3+} and V^{2+}). The reason is the stronger interaction between the more accessible 4d orbitals and the water ligands, possibly including a higher amount of d–p(OH_2) π-bonding involving the unoccupied $t_g(T_h)$ d-orbitals. This is also reflected in the experimental ligand field parameters $10Dq$; those for the trivalent ions are about twice as large as for the divalent 3d ions, and for the high-spin 4d Mo^{3+} ion, about 50% larger than for the 3d Cr^{3+} ion.[4a] The difference curve between the trivalent ions has a steeper slope than that for the divalent (Figure 3), consistent with the higher charge.

The binding energy of $[In(H_2O)_6]^{3+}$ appears to be lower than that anticipated from the trends in Figure 3, possibly an effect of the different type (all electron) of metal basis set used, even though the test calculations on Ag^{3+} did not reveal significant deviations from the ECP basis (see Methods). An additional difference is, however, that both the neutral Ga and In atoms have occupied valence p orbitals in their ground state, and thus low-lying unoccupied p orbitals are available to accept charge in the ionic state.

Table 5. CSOV Analyses of $[Sc(H_2O)_6]^{3+}$, $[Fe(H_2O)_6]^{3+}$, and $[Ga(H_2O)_6]^{3+}$

computation method	ΔE/kJ mol^{-1}	ΔE/%
$[Sc(H_2O)_6]^{3+}$		
1. Coulomb interaction between frozen systems	1769.4	73.02
2. H_2O polarization, frozen occupied Sc orbitals	419.1	17.29
3. M^{3+} relaxation, frozen H_2O(occ.)	0.5	0.02
4. charge transfer	229.2	9.46
5. full SCF	5.0	0.21
total SCF binding energy	2423.3	100
$[Fe(H_2O)_6]^{3+}$		
1. Coulomb interaction between frozen systems	2040.7	73.31
2. H_2O polarization, frozen Fe(occ. orbitals)	477.8	17.16
3. M^{3+} relaxation except Fe(3d), frozen H_2O(occ.)	0.13	0.005
4. H_2O optimized in full basis except Fe(3d)	90.3	3.24
5. Fe(3d) relaxation	34.2	1.23
6. optimized H_2O and Fe3d, frozen Fe(occ.)	138.6	4.98
7. full SCF	1.8	0.065
total SCF binding energy	2783.6	100
$[Ga(H_2O)_6]^{3+}$		
1. Coulomb interaction between frozen systems	2227.5	74.05
2. H_2O polarization, frozen Ga(occ. orbitals)	568.4	18.90
3. M^{3+} relaxation, frozen H_2O(occ. orbitals)	5.1	0.17
4. charge transfer	200.2	6.66
5. full SCF	7.0	0.23
total SCF binding energy	3008.2	100

Another point reflecting the stronger ligand field for the 4d elements is the binding energy correction ΔE_{CAS} for the contribution of the atomic ground state in the wave function, which is included for the d^2 and d^7 ions (see Methods).[1] The mixing of the different d-states should decrease with an increasing ligand field, and the corrections for the 4d ions are only about one-half as large as those for the 3d ions.

V. CSOV Analyses. Constrained space orbital variation[44] analyses have been performed on the hexahydrated Sc^{3+}, Fe^{3+}, and Ga^{3+} ions in order to examine the metal ion–water bonding in more detail. In this method the total binding energy at the SCF level is decomposed into the energy contributions obtained by successively increasing the space of orbital rotation. These calculations were performed without the most diffuse s, p, and d functions on the metals and with the medium-sized water basis set. The results from the different steps, which will be described in detail below, are given in Table 5.

The orbitals corresponding to an isolated M^{3+} ion and six free water molecules were first generated for the separated non-interacting systems. In the first step the ligands were moved from infinity to the bond distance (2.17, 2.05, and 1.99 Å, for Sc^{3+}, Fe^{3+}, and Ga^{3+}, respectively) with the occupied metal orbitals frozen and the virtual metal orbitals deleted. The energy obtained at the first SCF iteration gives a measure of the electrostatic ion-dipole attraction energy without charge relaxation. At convergence, the second step in Table 5, the water ligands are polarized in their virtual space, and the energy improvement corresponds to the electrostatic ion-induced dipole energy. In the third step, the occupied water orbitals thus obtained are frozen, the virtual water orbitals are deleted, and the metal ion is allowed to relax in its virtual space. The occupied metal orbitals are then frozen in the fourth step, where the water ligands are allowed to rotate in the full virtual space. In this step the charge transfer takes place. The energy gain obtained so far is finally compared with the full SCF energy. A minor final contribution, step five,

(44) Bagus, P. S.; Hermann, K.; Bauschlicher, C. W. *J. Chem. Phys.* **1984**, *80*, 4378.

Table 6. Mulliken Population Analyses: Metal Atom Charges and Orbital Populations in $[M(H_2O)_6]^{n+}$ Complexes[a] and Ionization Potentials, IP/eV[b]

M	q(M)	s	p	d	IP_{II}	IP_{III}
		Divalent 3d Ions				
Ca^{2+}	+1.94	6.04	11.89	0.14	11.87	
Sc^{2+}	+1.89	6.07	11.88	1.16	12.80	
Ti^{2+}	+1.88	6.10	11.90	2.12	13.58	
V^{2+}	+1.83	6.13	11.94	3.10	14.65	
Cr^{2+}	+1.76	6.16	12.04	4.04	16.50	
Mn^{2+}	+1.73	6.18	12.11	4.98	15.64	
Fe^{2+}	+1.68	6.21	12.14	5.98	16.18	
Co^{2+}	+1.62	6.23	12.18	6.97	17.06	
Ni^{2+}	+1.56	6.25	12.22	7.97	18.17	
Cu^{2+}	+1.52	6.26	12.25	8.97	20.29	
Zn^{2+}	+1.51	6.26	12.27	9.95	17.96	
		Trivalent 3d Ions				
Sc^{3+}	+2.47	6.16	11.86	0.51		24.76
Ti^{3+}	+2.44	6.21	11.86	1.48		27.491
V^{3+}	+2.34	6.27	11.91	2.48		29.31
Cr^{3+}	+2.21	6.32	12.01	3.46		30.96
Mn^{3+}	+2.11	6.37	12.16	4.36		33.667
Fe^{3+}	+2.05	6.42	12.30	5.24		30.651
Co^{3+}	+1.90	6.46	12.38	6.26		33.5
Co^{3+c}	+1.74	6.46	12.33	6.47		
Ni^{3+}	+1.76	6.49	12.46	7.29		35.17
Cu^{3+}	+1.64	6.61	12.14	8.32		36.83
Zn^{3+}	+1.53	6.53	12.62	9.32		39.722
Ga^{3+}	+1.95	6.38	12.45	10.22		30.71
		Divalent 4d Ions				
Sr^{2+}	+1.96	2.06	6.00	0.02	11.030	
Y^{2+d}	+1.74 (1.75)[e]	2.25	6.03	0.98	12.24	
Zr^{2+d}	+1.75 (1.78)[e]	2.11	5.93	2.20	13.13	
Nb^{2+}	+1.83	2.12	5.90	3.15	14.32	
Mo^{2+}	+1.86	2.12	5.93	4.09	16.15	
Tc^{2+}	+1.88	2.13	5.94	5.05	15.26	
Ru^{2+d}	+1.80 (1.78)[e]	2.16	5.97	6.07	16.76	
Ru^{2+c}	+1.74	2.19	5.84	6.21		
Rh^{2+}	+1.82	2.17	5.94	7.07	18.08	
Pd^{2+}	+1.69	2.19	5.92	8.12	19.43	
Ag^{2+}	+1.69	2.24	5.97	9.09	21.49	
Cd^{2+}	+1.72	0.14	0.11	10.03	16.908	
		Trivalent 4d Ions				
Y^{3+}	+2.43	2.14	6.02	0.41		20.52
Zr^{3+d}	+2.37 (2.42)[e]	2.19	6.01	1.43		22.99
Nb^{3+d}	+2.38 (2.44)[e]	2.19	5.98	2.45		25.04
Mo^{3+}	+2.41	2.21	5.94	3.44		27.16
Tc^{3+}	+2.38	2.22	6.00	4.41		29.54
Ru^{3+c}	+2.14	2.28	6.00	5.58		
Ru^{3+}	+2.35	2.27	6.05	5.33		28.47
Rh^{3+d}	+2.20 (2.25)[e]	2.29	6.09	6.42		31.06
Rh^{3+c}	+2.10	2.33	5.96	6.57		
Pd^{3+}	+2.11	2.32	6.07	7.50		32.93
Ag^{3+}	+1.90 (1.83)[f]	2.43	5.90	8.94		34.83
Cd^{3+g}	+1.86	0.32	0.26	9.57		37.48
In^{3+f}	+2.19	8.30	18.38	20.14		28.03

[a] Medium O/H basis set. [b] Reference 45b. [c] Low-spin, CAS calculations. [d] D_{3d} symmetry. [e] T_h symmetry. [f] All-electron calculation. [g] Large-core ECP.

Table 7. Low-Spin (d^8) Square-Planar Complexes, $[M(H_2O)_4]^{2+}$

M	R_4(M–O)/Å	q(M)	ΔE_4(CAS)[a,b]	δE[c]	ΔE_4(MRCI)[a,d]
Ni^{2+}	1.946	+1.404	996	66.6	1095
Pd^{2+}	2.072	+1.462	1048	76.0	1063
Ag^{3+}	1.976	+1.603	2195	81.3	

[a] $\Delta E_4 = E\{M^{2+}\} + 4E\{H_2O\} - E\{M(H_2O)_4\}$/kJ mol^{-1}. [b] CASSCF calculations with all 3d (4d) orbitals active. [c] Binding energy (CAS) compared with that for hexahydrate; $\delta E = \Delta E_4/\Delta E_6$ (%). [d] MRCI + Davidson correction, medium O/H basis, metal basis set extended with one f function, 3d (4d) orbitals correlated.

shows the polarization of the occupied metal orbitals. The steps mentioned offer a straightforward comparison of the binding energy contributions in the diamagnetic $[Sc(H_2O)_6]^{3+}$ and $[Ga(H_2O)_6]^{3+}$. However, for $[Fe(H_2O)_6]^{3+}$, a few additional steps have to be included, since the open 3d shell must be treated separately because only rotations between doubly occupied orbitals are energy invariant. The first four steps are similar to those for $[Sc(H_2O)_6]^{3+}$ and $[Ga(H_2O)_6]^{3+}$ but without relaxing the 3d orbitals, which until this point thus have the same form as in Fe^{3+} (the mixing of d_{z^2} and $d_{x^2-y^2}$, both of A_1 symmetry as the calculations were performed in the D_{2h} subsymmetry, is formally allowed but should make a negligible energy contribution). For $[Fe(H_2O)_6]^{3+}$, in the fifth step, the 3d orbitals are allowed to rotate in the full virtual space, giving an additional term for the M^{3+} relaxation. In the sixth step (corresponding to the fourth, the charge-transfer step for Sc^{3+} and Ga^{3+}), the water molecules were allowed to relax in the full virtual space and the result was then finally compared to the full SCF energy.

The results of the CSOV analyses do not show any conclusive difference between Ga^{3+} and the other ions. The energy gains in the first step approximately follow an R^{-2} dependence, as expected for a charge–dipole interaction, and for the second step, an R^{-4} dependence for a polarization energy ($E = -^1/_2\alpha_{zz}(ze)^2/r^4$). The M^{3+} relaxation energy is largest in $[Fe(H_2O)_6]^{3+}$ (0.13 + 34.2 kJ mol^{-1}). The corresponding amount is greater for $[Ga(H_2O)_6]^{3+}$ (~5 kJ mol^{-1}) than for $[Sc(H_2O)_6]^{3+}$ (0.5 kJ mol^{-1}), reflecting the more pronounced tendency for a 3d–4s mixing in $[Ga(H_2O)_6]^{3+}$ as compared to the harder valence shell in $[Sc(H_2O)_6]^{3+}$.

VI. Low-Spin States. One consequence of the larger ligand field splittings for the 4d ions, and also for the trivalent ions, is that low-spin ground-state complexes are formed by several of the hydrated ions in this study (Co^{3+}, Ru^{2+}, Ru^{3+}, Rh^{3+}, Pd^{2+}) as shown, for example, by UV–vis spectroscopy.[8] The $4d^5$ complex $[Ru(H_2O)_6]^{3+}$ is low-spin, while its $3d^5$ counterpart, $[Fe(H_2O)_6]^{3+}$, is high-spin. The d^6 ions, Co^{3+}, Rh^{3+}, and Ru^{2+}, all have singlet ground states in hexaaqua complexes.

As shown above, calculations at the SCF level yield results for the hexaaqua clusters, allowing satisfactory comparisons of most systematic trends when only high-spin states are compared. However, the SCF high-/low-spin comparisons in Table 3 show that only Rh^{3+} is correctly predicted to be low-spin in its ground state. The large water basis set did not improve the results. Evidently, too low binding values are obtained for the low-spin complexes with this model. Calculations with methods including electron correlation reduce the energy difference, especially for the small ions (Table 3). In particular, addition of an f function to the metal basis proved to be important for the correlation treatment. For Fe^{2+}, the divalent ion in the first transition period which should have the largest tendency to form low-spin complexes, the atomic separation between the ground ^5D (j-averaged) and the excited ^1I state has been measured to be 29 933.3 cm^{-1}.[45] The corresponding calculated excitation energy values are 41 636 (SCF) and 33 282 cm^{-1} (MRCI with 3d correlated + Davidson correction); the latter is only 3349 cm^{-1} (40 kJ mol^{-1}) above the experimental value. The corresponding difference is 39 kJ mol^{-1} for the $^5D \rightarrow {}^3P$ transition of Cr^{2+}. These comparisons illustrate that a large part of the remaining energy difference between the high- and low-spin states is due to the metal atom description. If corrections of this size would be introduced for all ions in Table 3, only the gas-phase clusters of Ru^{3+} and Co^{3+} would still have slightly lower energy in high-spin. However, it seems probable that the hydrogen bonding to the second shell, which should be stronger for the smaller low-spin ions and thus give a synergistic increase in the strength of the M–O bonds and in the ligand field, plays an important role for these ions, although the proposed transition to low-spin of Cr^{2+} in its $[Cr(H_2O)_6]SiF_6$ salt requires an even larger contribu-

(45) (a) Moore, C. E. *Atomic Energy Levels*; National Bureau of Standards: Washington, DC, 1971. (b) Moore, C. E. *Ionization Potentials and Ionization Limits Derived from the Analysis of Optical Spectra*; NSRDS-NBS 34; U.S. National Bureau of Standards: Washington, DC, 1970.

tion from the surroundings (see Jahn–Teller Effects in Hexaaqua Ions, above).

VII. Mulliken Population Analyses. The variations of the metal ion charges in the high-spin hexaaqua complexes according to Mulliken population analyses are compared in Table 6 with values obtained using the medium-sized water basis set. Clear trends are evident from the comparisons showing an increasing charge transfer to the right in the series consistent with an increased covalency of the M–O bonds. It seems likely that the transfer of more than one electron charge for the trivalent hexahydrated Ni^{3+}, Cu^{3+}, Zn^{3+}, Ag^{3+}, and Cd^{3+} ions, is related to their instability toward the +II oxidation state. At the end of the series the stable d^{10} ions Ga^{3+} and In^{3+} break the trends with a smaller charge transfer. A more irregular pattern is found for the charge transfer to the divalent high-spin 4d ions in hexaaqua complexes. The orbital populations show, however, that the s orbitals receive the main part while the p and d orbitals are close to their formal occupation numbers (Table 6). A generally low involvement of the p orbitals is also found for the trivalent 4d ions, notable even in a comparison with the divalent 3d ions.[1a]

Considering the similarity of the hydrogen bond strengths for series of hydrated metal ions in solution as measured by the O–D stretching vibration frequencies of the water ligands,[1,46] the small variations found in the charge on the H atoms within each series (±0.02) are noteworthy, although the O–D frequency should also be influenced by the larger concurrent variations in the oxygen charge, cf., for example, Table III in ref 1a.

The ionization energies of the metal ions[45b] are given in Table 6. The unstable trivalent ions with a high charge transfer correspond to high third ionization potentials. The binding energies are found to be approximately linearly correlated with the ionization energies, probably because the coordination of polar ligands would have an effect similar to the addition of electrons, as discussed in a previous study.[1a]

VIII. Square-Planar d^8 Complexes. The two hydrated divalent d^8 ions Ni^{2+} and Pd^{2+} display strikingly different behaviors. While Ni^{2+} forms regular and stable octahedral hydrates, Pd^{2+} coordinates four water molecules in square-planar low-spin complexes.[11] This difference can be explained by ligand field theory. In a weak octahedral field, a d^8 ion must have a triplet ground state with two electrons with parallel spins in the $e_g(O_h)$ orbital. However, if two axial ligands are removed from the system, giving a square-planar configuration of D_{4h} symmetry, the ligand field splits the e_g orbitals into a pair with a_{1g} and b_{1g} symmetries. For a strong D_{4h} ligand field this energy gain may be sufficient to stabilize a square-planar low-spin geometry. The other possible explanation is that the water ligands donate charge to the hydrated palladium(II) ion such that it attains a Jahn–Teller unstable d^9 electron configuration, which would distort toward a square-planar geometry. For Pd^{2+} this is not likely because the charge in the low-spin square-planar configuration is +1.46 (Table 7), compared with +1.69 for both palladium(II) and silver(II) in high-spin hexaaqua clusters (Table 6). Furthermore, the orbital populations show almost eight d-electrons in the 4d shell for palladium(II). In the low-spin d^8 $[Ag(H_2O)_4]^{3+}$ complex, however, the charge of the silver(III) ion is reduced to +1.6 (Table 7), with a d-orbital population close to 9. The square-planar structure of silver(III) could therefore alternatively be described as a result of a strong Jahn–Teller distortion although, as discussed above, an extensive charge transfer should be connected to redox instability. A high acidity would be expected of the strongly polarized water ligands of the hydrated Ag(III) ion, as evidenced by the occurrence of the $[Ag(OH)_4]^-$ complex in solution.[25]

The SCF-level binding energies of the square-planar complexes have been compared to those of the corresponding hexahydrates, see Table 7. The higher stability of the 4d tetrahydrates is shown by the larger relative binding energies of the Pd^{2+} and Ag^{3+} ions (~76 and 81% of ΔE_b of the hexahydrate, respectively) compared to Ni^{2+} (~66%). Consequently, there seems no reason to doubt that the hydrated silver(III) ion would attain a square-planar structure.

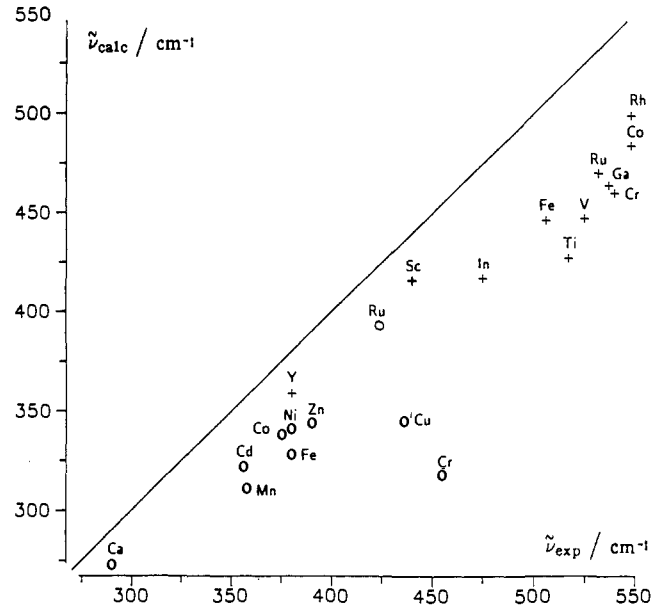

Figure 5. Vibrational symmetric stretching frequencies (cm^{-1}) calculated for the hexahydrated divalent ions Ca^{2+}, Cr^{2+}, Mn^{2+}, Fe^{2+}, Co^{2+}, Ni^{2+}, Cu^{2+}, Zn^{2+}, Ru^{2+}, and Cd^{2+} (circles) and the trivalent ions Sc^{3+}, Ti^{3+}, V^{3+}, Cr^{3+}, Fe^{3+}, Co^{3+}, Ga^{3+}, Y^{3+}, Ru^{3+}, Rh^{3+}, and In^{3+} (crosses) plotted against experimental Raman values (Table 1).

IX. Vibrational Frequencies. The symmetric (A_g) stretching vibrational frequency ν_s of the hexahydrated complexes is directly connected to the strength of the metal–oxygen bond because of the stationary metal atom. The wave number $\tilde{\nu}_s$ is immediately available in the harmonic approximation as a result of the optimization of the M–O distance and is obtained from $\Delta E_{vib} = f(\Delta x)^2 = hc\tilde{\nu}_s$, with the normal coordinate $\Delta x = [6(\Delta R)^2]^{1/2}$, the force constant $f = 4\pi^2\mu\nu^2$, and the reduced mass μ equal to the mass of the ligand. A parabolic function has been fitted to three points: one very close to r_e (within 0.01 Å) and two approximately ±0.04 Å off-minimum. However, the calculated frequencies are sensitive to the choice of fitting points because of the anharmonicity,[47] and the uncertainty is estimated to be ±10 cm^{-1}. On the other hand, test optimizations on the Mn^{2+} and Fe^{3+} systems showed that the choice of the water basis set had a negligible influence.

The calculated values are compared with the experimental ones obtained from Raman spectra of hydrated metal ions in solution and in some cases in alum salts (Table 1). Calculated SCF frequencies are generally overestimated by ~10% for molecules in the gas phase with a high degree of covalency[47,48] due to the incorrectly described dissociation within the restricted Hartree–Fock SCF approximation. However, in solution, the dissociation is to ions and we find the HF-SCF description to give a rather constant deviation in the range of 10–15% with *lower* theoretical than experimental frequencies for the symmetric stretching vibration mode (Figure 5). The difference is approximately 30–50 cm^{-1} for the divalent ions (larger for the Jahn–Teller ions Cu^{2+} and Cr^{2+}) and 60–80 cm^{-1} for the trivalent ions. This discrepancy is probably mostly due to the solvation effects, e.g. the hydrogen bonding enhances the polarization of the water ligands and thereby leads to increased experimental frequencies.

(46) (a) Bergström, P.-Å.; Lindgren, J.; Read, M.; Sandström, M. *J. Phys. Chem.* **1991**, *95*, 7650. (b) Bergström, P.-Å.; Lindgren, J. *Inorg. Chem.* **1992**, *31*, 1529 and references therein.

(47) Hehre, W. J.; Radom, L.; Schleyer, P. v. R.; Pople, J. A. *Ab Initio Molecular Orbital Theory*; Wiley-Interscience: New York, 1986; Chapter 6.3.

(48) Del Bene, J. E.; Mettee, H. D.; Frisch, M. J.; Luke, B. T.; Pople, J. A. *J. Phys. Chem.* **1983**, *87*, 3279.

Also, anharmonicity and the "wall effect" due to the surrounding molecules are not present in the gas-phase vibrational frequency calculations and should contribute to the increase.

The smaller deviations for Ca^{2+} and Sc^{3+}, calculated to be only ca. 17 and 24 cm^{-1} lower than the experimental values (Table 1), respectively, are probably caused by low experimental frequencies because of hydration numbers higher than six.[1,14,16,36] Already for the heptahydrates, $[Ca(H_2O)_7]^{2+}$ and $[Sc(H_2O)_7]^{3+}$, the calculated symmetric stretching wave numbers are substantially reduced to ν_s = 222 and 373 cm^{-1}, respectively. These values were obtained by moving the water molecules along the coordinate $\Delta x = [7(\Delta R)^2]^{1/2}$ while keeping the angular coordinates (α and β) fixed, see Figure 1 in ref 31. The smaller than average difference for Y^{3+}, 21 cm^{-1}, can likewise be related to an experimental hydration number of 8.0 ± 0.3.[17]

The spread around a correlation line through the points in Figure 5 would probably be reduced by comparing the calculated frequencies with a weighted sum of all three experimental stretching vibrations (of A_{1g} (×1), E_g (×2), and T_{1u} (×3) symmetry in the O_h point group) in order to eliminate the interaction force constants,[49] i.e. the influence of the interactions between the ligands on the experimental frequency in the comparison, but experimental values are missing in most cases.

X. Gas-Phase and Solution Hydration Enthalpies. The calculated binding energy, ΔE_b, refers to a gas-phase (de)-hydration reaction of a metal ion at 0 K, $M(H_2O)_6^{n+}(g) \rightarrow M^{n+}(g) + 6H_2O(g)$, and a number of contributions have to be considered in order to relate this quantity to experimental single-ion hydration enthalpies, $\Delta H°_{hyd}$, at 298 K.[29,48]

Firstly, the hydration enthalpy for the gas-phase hydration reaction at 298 K, ΔH_{gas}, should be obtained from the binding energy, ΔE_b at 0 K.[48] The difference in vibrational zero-point energy in forming a complex, ΔE_{zp}, gives a relatively constant reduction of ΔE_b by about 60–70 kJ mol^{-1} in the series.[29] The adjustment to 298 K corresponds to an additional small reduction of about 5 kJ mol^{-1} for the difference in heat capacity of the components of the system, $\Delta E(C_p)$.[50] The gas law relates the so-corrected binding energy ΔE_b^{298} and the enthalpy ΔH_{gas} terms of the reaction at 298 K, $\Delta H_{gas} = \Delta nRT - \Delta E_b^{298}$,[48] with $\Delta nRT \approx 15$ kJ mol^{-1} for six water molecules. For the 3d elements, relativistic effects have been neglected but should give rise to a correction, ΔE_{rel}, with increased binding energies in particular for the elements with higher 4s populations toward the right in the row. Comparisons can be made with a model study of the mono- and dihydrated divalent ions of the 3d ions Ca^{2+}–Zn^{2+}, where the relativistic effects were evaluated quantitatively for the large O/H basis set.[51] At the SCF level the binding energies were found to increase by 1–10 kJ mol^{-1}. Perturbation theory estimates of the relativistic corrections for the hexahydrated 3d ions Ti^{2+}, Fe^{2+}, and Zn^{2+} increased the binding energy with ~4, ~6, and ~11 kJ mol^{-1}, respectively. From these results, the $[Ga(H_2O)_6]^{3+}$ ion, with a large s population (6.28 with the large water basis set), is estimated to have a relativistic contribution of about 20 kJ mol^{-1} to the binding energy.

Relativistic corrections are included in the ECP basis sets for the 4d elements. The all-electron calculations for Ag^{2+} and In^{3+} revealed, as expected, that the inherent relativistic effects are much larger than those for the 3d ions, both energetically and geometrically. Thus, the nonrelativistic binding energies were smaller than the relativistic (see Table 4) by 28 and 50 kJ mol^{-1} for Ag^{3+} and In^{3+}, respectively, while the M–O distances were approximately 0.01 Å longer.

The effect of differences in the spin–orbit coupling between the free metal ion[45] and the complex is estimated to give a small reduction of the binding energies, ΔE_{so}, on the order of 5–10 kJ mol^{-1}.

Structure determinations of water molecules in crystals by neutron diffraction show that on the average the HOH angle opens up a few degrees upon coordination to a metal ion.[39a] Optimizations performed for the divalent mono- and dihydrates (large water basis) of the 3d ions indicate that this effect increases with the increasing covalent bonding contribution for the late transition elements.[51] Using the optimized water geometry from the monohydrates for calculations on the hexahydrates of Cu^{2+} and Zn^{2+}, ΔE_{geom} contributions to the binding energy of about 15 and 20 kJ mol^{-1}, respectively, were obtained. The large water basis should give smaller effects, as also was indicated by test calculations.

Corrections due to the lack of electron correlation in the SCF approximation have been estimated by MP2 methods for the hexaaqua clusters of Mn^{2+}, Co^{2+}, Zn^{2+}, and Cd^{2+}.[29] The contributions to the binding energy were reported to be ΔE_{corr} = 28.5, 36.4, 19.7, and 28.9 kJ mol^{-1}, respectively, with an anomalously large value for cobalt(II). For the Co^{2+} ion, however, a two-configuration reference wave function is required (see Methods), which explains the deviation of the MP2 result for this system.

For a comparison with experimental $\Delta H°_{hyd}$ data, the most important contribution by far is to relate the gas-phase binding energies to the state in solution, where effects of the surroundings become important. Using a Born–Haber cycle, as shown before,[1] the following relation is obtained for the (corrected) gas-phase hydration enthalpy at 298 K:

$$\Delta H_{gas} = \Delta H°_{hyd} - \Delta H_6^{solv} - 6\Delta H_{vap} \qquad (2)$$

where the heat of vaporization of water is ΔH_{vap} = 44.02 kJ mol^{-1} at 298 K.[52] Rough estimates of the (negative) solvation term ΔH_6^{solv}, corresponding to $[M(H_2O)_6(g)]^{n+} \rightarrow [M(H_2O)_6(aq)]^{n+}$, can be made by approximate models, e.g. by the Born equation in which the ion is located in a cavity surrounded by a dielectric continuum.[43] This model has been reported to give reasonable energy values for a cavity radius obtained by adding ca. 1.5 Å to the M–O distance in hexahydrated ions.[29]

Including the results from the previous study on the hexahydrated divalent 3d ions of the first transition period (Ca^{2+}–Zn^{2+}),[1] there are totally 28 experimental single ion hydration enthalpies, $\Delta H°_{hyd}$, which may be compared with theoretical ΔE_b values (Table 4). The data form two groups with much higher hydration enthalpies for the trivalent ions, as expected from the q^2/r dependence of the solvation energy in the Born equation.[43]

In Figure 6 the expression $\Delta H°_{hyd} + \Delta E_b - 6\Delta H_{vap}$ is plotted for the 3d ions. This should give a good estimate of the solvation energy $\Delta H_6^{solv} = \Delta H°_{hyd} - \Delta H_{gas} - 6\Delta H_{vap}$ if the above-mentioned corrections are accounted for, i.e.

$$\Delta E_b = -\Delta H_{gas} - \Delta E_{zp} + \Delta nRT - \Delta E(Cp) + \Delta E_{rel} - \Delta E_{so} + \Delta E_{geom} + \Delta E_{corr} \qquad (3)$$

For the divalent 3d ions, the estimated corrections seem to largely cancel (within ca. ±30 kJ), and rather constant ΔH_6^{solv} values, in the range from 926 kJ mol^{-1} for Mn^{2+} to about 1020 kJ mol^{-1} for Ni^{2+} and Cu^{2+}, are obtained if Ca^{2+} is excluded (because of its higher hydration number).[1a] The corresponding ΔH_6^{solv} values are larger for the trivalent 3d ions, in the range from 2096 for Ti^{3+} to ca. 2256 kJ mol^{-1} for both Cr^{3+} and Mn^{3+}, excluding the values for Sc^{3+} and Co^{3+} because of higher hydration number and low-spin, respectively. Considering the uncertainties in the comparisons, the overall differences in hydration energy between

(49) Jones, L. H. *Inorganic Vibrational Spectroscopy*; Marcel Dekker: New York, 1971; Vol. 1, Chapter 3.2.
(50) Mhin, B. J.; Lee, S.; Cho, S. J.; Lee, K.; Kim, K. S. *Chem. Phys. Lett.* **1992**, *197*, 77.
(51) Åkesson, R.; Pettersson, L. G. M. *Chem. Phys.*, in press.
(52) *American Institute of Physics Handbook*; Gray, D. E., Ed.; McGraw-Hill: New York, 1972.

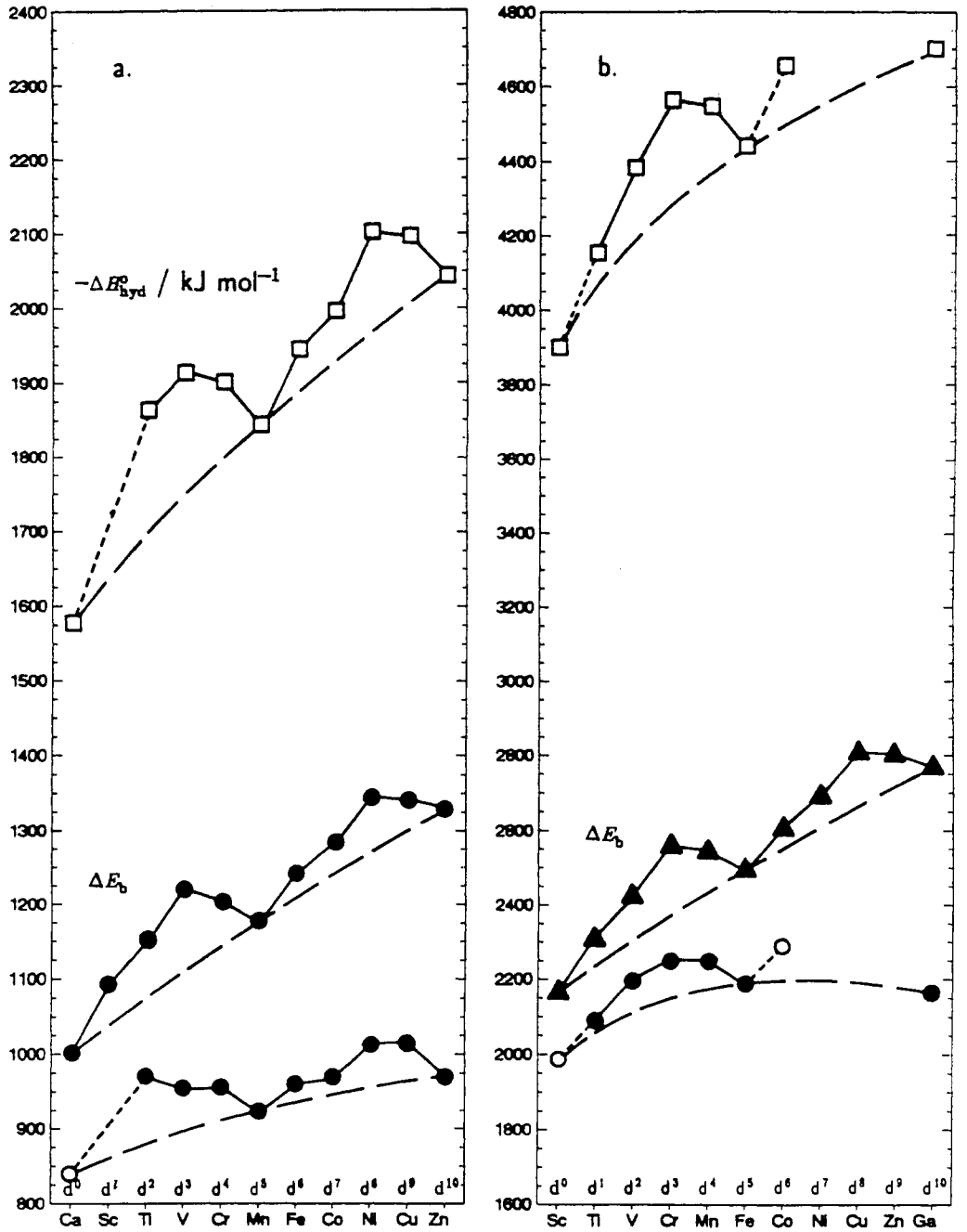

Figure 6. Experimental single-ion hydration enthalpies, $-\Delta H^{\circ}_{hyd}$ (upper curve), theoretical binding energies, ΔE_b (middle curve), and $-(\Delta H^{\circ}_{hyd} + \Delta E_b - 6\Delta H_{vap}) \approx -\Delta H_6^{solv}$ (lower curve) in kJ mol^{-1} for the 3d elements: (a) divalent ions and (b) trivalent ions (note: scale/2). The reference curves (dashes) connect d^0, d^5, and d^{10} ions. The ΔH°_{hyd} values of Ca^{2+} and Sc^{3+} correspond to higher hydration numbers and Co^{3+} to low-spin (see text).

the 3d and the 4d $[M(H_2O)_6]^{n+}$ complexes can be accommodated within the simple description leading to the Born equation.[43]

In this context results from liquid XPS studies of metal ions in glycol solution are of interest.[53] The fast core excitation process when the charge is increased for the same radius of the complex has been used to show that the electronic polarization is the dominating contribution to the increase in solvation energy. In contrast to the linear increase of the long-range ion-dipole term with increasing charge, the electronic polarization increases quadratically as is expected from the Born model.

However, it seems from the curves in Figure 6 that the ligand field induced *variations* in the hydration enthalpies are larger than in the calculated binding energies, especially for the trivalent ions. This would be consistent with a further enhancement of the ligand field from the surrounding coordination spheres which would stabilize the low-spin state for trivalent ions in solution, not only for Co^{3+} but also for the 4d ions Ru^{3+} and Rh^{3+}. IR spectroscopic measurements of O–D (O–H) stretching frequencies have shown that the hydrogen bond strength is almost constant for most divalent transition ions in solution but increases stepwise to another constant value for small trivalent ions, e.g. Cr^{3+} and Rh^{3+}, for which even the hydrogen bonds between the second and third hydration layers are enhanced.[46]

Concluding Remarks. In the present study we have evaluated the ligand field effects on the high-spin states of the di- and trivalent hexahydrated ions of the first and second transition periods. Energy gains and geometrical distortions by additional splitting of degenerate d orbitals have been considered. The almost linear correlation between the binding energies, ΔE_b, and the inverse M–O bond distances, R^{-1}, shows that the bonding in the divalent complexes is dominated by electrostatic effects in both

(53) Siegbahn, H. *J. Phys. Chem.* **1985**, *89*, 897.

periods. The stronger ligand field effects in the second period are shown by the larger variations of the energy curves, giving more marked maxima for the d^3 and d^8 ions in the series. The trivalent ions form bonds with more covalent contributions, which is reflected in the much larger variation in the metal atomic charges as obtained from the Mulliken population analyses, and a connection between extensive charge transfer and instability of the high oxidation state is pointed out.

The low-spin ground states of the hydrated Co^{3+}, Ru^{2+}, Ru^{3+}, Rh^{3+}, and Pd^{2+} ions, and also the possibility of a low-spin state of Cr^{2+} in the solid $[Cr(H_2O)_6]SiF_6$ compound, have been considered. The low-spin square-planar structure for the tetrahydrated divalent palladium ion is explained in terms of ligand field effects, and the hydrated Ag^{3+} ion is predicted to have the same structure. The hydrated Ag^{2+} ion is probably a hexahydrated Jahn–Teller distorted $[Ag(H_2O)_6]^{2+}$ complex with a tetragonally elongated structure similar to that for the Cu^{2+} ion. It is evident, however, that low-energy distortions induced by the electronic structure, e.g. Jahn–Teller effects and conformation changes, can easily be suppressed or otherwise influenced in crystal structures due to packing forces and caution is required particularly in structural comparisons using solid-state data.

Comparisons with experimental bond lengths, symmetric stretching vibrational frequencies, and single-ion hydration enthalpies are used for discussions of changes in hydration numbers, structure, and spin states and also to illuminate the expected influence of the surrounding hydrogen-bonded medium in solution and in the solid state.

Lately, computational models have been developed to describe the solute under the influence of a polarizable dielectric continuum.[54-56] An interesting attempt was made to describe the solvent effects on some hexahydrated ions, including Ca^{2+} and Zn^{2+}, by reoptimizing the hexahydrated ion inside a cavity in a continuum with the dielectric permittivity of water.[56] However, despite the reasonable energy contributions obtained from the continuum, albeit with rather large radii of the cavities, the M–O bond lengths increased significantly, by 0.02–0.05 Å, and the M–O stretching force constants decreased substantially from the gas-phase values obtained in the same work, i.e. contrary to the expected effects. It seems that the size of the supermolecule inside the cavity must be rather large particularly when strong hydrogen bonding occurs, as discussed in ref 55. In the case of the extremely strong hydrogen bonding around small trivalent ions, such as Cr^{3+} and Rh^{3+},[46] probably at least the second hydration shell should be included for a satisfactory description. Additional problems arise when using the cavity model for Jahn–Teller distorted complexes with different strengths of the hydrogen bonds and possibly also different tilt angles of the axial and equatorial water ligands,[2,3] or for square-planar complexes, as the size and shape of the cavity may have a significant influence on the results.[55] Nevertheless, with the rapidly developing computational capacity for accurate descriptions of large systems, the supermolecule and cavity approach will certainly become a useful method for quantitative evaluations not only of hydration energies but also of the geometrical effects occurring upon the hydration of metal ions.

Acknowledgment. The financial support and the CPU time on a CRAY X-MP/416 computer, obtained from the Swedish Natural Science Council, is gratefully acknowledged. Professor F. A. Cotton is thanked for preprints and stimulating discussions.

(54) Cramer, C. J.; Truhlar, D. G. *Chem. Phys. Lett.* **1992**, *198*, 74 and references therein.

(55) Tuñón, I.; Silla, E.; Bertrán, J. *J. Phys. Chem.* **1993**, *97*, 5547 and references therein.

(56) Sánchez Marcos, E.; Pappalardo, R. R.; Rinaldi, R. *J. Phys. Chem.* **1991**, *95*, 8928.